

Unlocking Choline Dihydrogen Citrate as a New Potential Hydrogen Bond Acceptor Replacing Choline Chloride in Malonic Acid-Based Deep Eutectic Solvent Formulation

Mohammad Amin Wan Chik¹, Muhammad Hakimin Shafie², Roziana Mohamed Hanaphi¹ and Rizana Yusof^{1*}

¹Faculty of Applied Sciences, Universiti Teknologi MARA, Cawangan Perlis, Kampus Arau, 02600 Arau, Perlis, Malaysia

²Analytical Biochemistry Research Centre (ABrC), University Innovation Incubator (I²U), sains@usm Campus, Universiti Sains Malaysia, Lebuh Bukit Jambul, 11900 Bayan Lepas, Penang, Malaysia

*Corresponding author (e-mail: rizana@uitm.edu.my)

The majority of deep eutectic solvents (DESs) are commonly synthesized utilising choline chloride (ChCl) as the hydrogen bond acceptor (HBA) due to its compatibility with a wide range of hydrogen bond donors (HBDs). However, depending solely on ChCl imposes constraints on the attainable properties suitable for specific industrial and research purposes. Therefore, choline dihydrogen citrate (ChDHCit) was chosen as new HBA to rival ChCl in the formulation of malonic acid (MA) based DESs. Note that the DESs were established at a mole ratio of 1:2 for further investigation of their physicochemical properties. FTIR-ATR analysis confirmed the formation of hydrogen bonds within both DES, with some significant C-O shifts observed in ChDHCit:MA. The complex anion $C_6H_5O_7^-$ in ChDHCit:MA caused more spectral shifts in FTIR compared to the anion Cl^- in ChCl:MA. Thermal analysis by TGA proved that ChDHCit:MA is less chemically stable against decomposition with a T_d value (227.85°C) lower than that of ChCl:MA (305.26°C) owing to their large anions. The high melting temperature (T_m) of ChDHCit:MA compared to that of ChCl:MA is due to factors such as strong intermolecular forces or less-ordered crystal structures. The hydrogen bonds formation in the DES was confirmed by FTIR-ATR, DSC, and TGA analyses. ChDHCit:MA was found to be less acidic, more viscous, and less dense, with higher surface tension and lower ionic conductivity than ChCl:MA because of the less stable malonate anion, non-symmetrical size of the $C_6H_5O_7^-$ anion, and low ion mobility. In conclusion, the complex anions in HBA changed the physicochemical properties of DES.

Keywords: Deep eutectic solvents; choline chloride; choline dihydrogen citrate; malonic acid; viscosity; density

Received: September 2024; Accepted: December 2024

In recent decades, ionic liquids (ILs) have received substantial research attention caused by their distinctive properties, including minimal volatility, greater thermal stability, strong polarity, greater ionic conductivity, broad liquid range, and customisability [1, 2]. However, ILs have disadvantages due to their cost, toxicity, and preparation methods [3-5]. Hence, deep eutectic solvents (DESs), which are third-generation ILs, are preferable because they are convenient to prepare, non-toxic, biodegradable, and have low melting points [6, 7]. DESs are structurally distinct from ILs with respect to their material and interactions. ILs are typically created through ionic bonds between heterocyclic cations and inorganic or organic anions, whereas DESs are prepared through hydrogen bonding between hydrogen bond acceptors (HBAs) as well as donors (HBDs) [7, 8].

DES consists of four types, which are Type I, Type II, Type III as well as Type IV. Type I to Type III

DES utilise quaternary ammonium salts as their primary component, which combined differently with metal salts, metal chlorides, and hydrogen bond donors (HBD), respectively. Conversely, Type IV DES consist of metal salts combined with HBD. Among these, Type III has been the most widely researched in literature and is typically based on choline chloride as the HBA, paired with various HBDs derived from carboxylic acids ($-COOH$), alcohols ($-OH$), and amines ($-NH_2$) [9, 10, 11]. Malonic acid (MA)-based DES is one of the examples of this Type III DES. The choice of MA as the DES component is due to its low acute toxicity. According to safety data sheet provided by Sigma-Aldrich, the LD50 (acute toxicity) of MA is 3250 mg/kg when tested to a rat. It is known that the lower the LD50 value (<5 mg/kg), the more toxic the substance, as smaller amount is needed to cause death in 50% of the population [12]. Since the LD50 value of MA is large, incorporating it as a component of DES is relatively harmless in various field. For

example, the use of this Type III DES as reaction media and catalysts in organic synthesis and biomass conversion [6, 13, 14], solvents for natural products extraction [6, 13], electrolytes in batteries and supercapacitors [6, 14], transdermal drug delivery [15], and water treatment processes [16].

The characteristics of DES are greatly affected by numerous factors, for example, the choice of components, HBA and HBD. ChCl is commonly employed as an HBA and is preferred for its compatibility with a wide range of HBDs. However, it is crucial to compare choline chloride (ChCl) with other types of HBAs in order to expand the potential and versatility of new DES system. Moreover, according to the safety data sheet provided by Sigma-Aldrich, ChCl has an LD50 value of 3900 mg/kg, whereas choline dihydrogen citrate (ChDHCit) has an LD50 value of 4800 mg/kg. This indicates that ChDHCit is considered less toxic than ChCl, thereby providing an opportunity for ChDHCit to serve as a new HBA that is safer and less harmful for use as a component in DES formulations. As a result, ChDHCit was chosen as a new HBA to compete with ChCl, with malonic acid (MA) as its partner. Thus, this study's objective was to examine the impact of different HBAs, namely ChCl and ChDHCit, on the properties of MA-based DES. It is hypothesised that the HBA within the DES system affects the physicochemical properties of the resulting eutectic. Consequently, both DES systems (ChCl:MA and ChDHCit:MA) were assessed in terms of acidity, density, surface tension, solubility, viscosity, ionic conductivity, functional groups, melting point, glass transition, crystallisation, and decomposition temperature to determine their suitability for various industries.

EXPERIMENTAL

Chemicals and Materials

Choline chloride (<98% purity: $C_3H_{14}NOCl$), choline dihydrogen citrate (<98% purity: $C_{11}H_{21}NO_8$), and malonic acid (purity 99%: $C_3H_4O_4$) were purchased from Sigma-Aldrich located in Saint Louis, USA. The chemicals, being of analytical grade, were kept in a desiccator to prevent moisture absorption.

Deep Eutectic Solvent (DES) Preparation

DES preparation was adapted and modified from a past study conducted by Shafie et al. [17]. DES was synthesized by combining two different HBAs (ChCl and ChDHCit) with an HBD (MA) in a 1:2 molar ratio, resulting in the formation of ChDHCit and ChCl. The mixture was stirred and heated to 80°C until a colourless liquid appeared. It was then left at room temperature for 24 h to confirm the absence of any precipitate. Afterward, the DES was stored in a desiccator to avoid moisture absorption.

Characterisation of DES

Polarised Light Microscopy (POM) Analysis

Visual analysis was conducted at 25°C employing an Olympus transmission microscope (CX21, Olympus, Japan) coupled with Infinity Analyzer Software and Lumenera Infinity camera. A droplet of each type of DES (ChCl:MA and ChDHCit:MA) was put on a microscope slide with a coverslip to cover the sample, prevent it from evaporating, and to keep it flat. The camera settings (1080 p × 60 fps) were adjusted to optimise the image quality. NIS-Elements software was used to capture images of the sample at magnifications 10x to record any observations or changes in the sample appearance. The images were analysed based on the surface and presence of crystals in both DES samples [17-19].

Fourier Transform Infrared-attenuated Total Reflectance (FTIR-ATR) Analysis

The analysis was performed using Fourier transform infrared-attenuated total reflectance (FTIR-ATR) (Fortier, PerkinElmer, USA) to determine the functional groups present in pure ChCl, ChDHCit, MA, and a eutectic mixture of ChCl:MA (1:2) and ChDHCit:MA (1:2). Prior to scanning, the ATR crystal was wiped with acetone using soft tissue paper to eliminate any residues or debris. The sample was placed directly and pressed (± 90 gauge) onto the ATR crystal to ensure a good contact. The samples were scanned four times in the 600–4000 cm^{-1} range [17].

Thermogravimetric (TGA) Analysis

The decomposition temperatures (T_d) of ChCl, ChDHCit, MA, ChCl:MA (1:2), and ChDHCit:MA (1:2) were determined using thermogravimetric analysis (TGA) TGA4000. The samples (10 mg) were loaded into a platinum crucible and heated at a 10°C·min⁻¹ rate from 30 to 900°C under nitrogen flow (60 mL·min⁻¹) [17,20]. The TGA instrument recorded the weight change of the samples as the temperature function. T_d was determined by determining the inflection point or temperature at which the sample showed significant weight loss due to decomposition.

Differential Scanning Calorimetry (DSC) Analysis

Differential scanning calorimetry (DSC) (DSC 6, Perkin Elmer, USA) was utilized to determine the melting point (T_m), glass transition temperature (T_g), and crystallisation temperature (T_c) of ChCl, ChDHCit, MA, ChCl:MA (1:2), and ChDHCit:MA (1:2) at a flow rate of 40 mL/min under a constant stream of nitrogen. Note that the samples were prepared, weighed to approximately 10 mg, and

securely sealed in aluminum pans while being heated at a rate of 5°C/min at temperatures ranging from -50 to 300°C [17, 21]. Once the sample was loaded, the temperature was gradually increased and the heat flow changes as a function of temperature were noted. To observe the T_m of the sample from the DSC curve, the peak temperature of the endothermic transition was identified using the TA instrument software (TA Instruments Universal Analysis 2000).

pH Determination

A pH meter was utilised to determine the pH of each liquid DES (ChCl:MA and ChDHCit:MA). The pH meter was calibrated at 25°C with buffer solutions of pH 4 and 7. The electrode was dipped into the DES samples, and the pH was recorded after the reading was constant for a few seconds. It was ensured that the electrode did not touch the bottom of the beaker, which could cause inaccurate readings. The pH readings were recorded in triplicate to obtain an average value [22]. The electrode was subsequently washed with distilled water and dried with a clean tissue.

Viscosity Measurement

A viscometer (Brookfield DV-I Prime, USA) fitted with a water bath under a digital hotplate was used to determine the viscosity of the DES (ChCl:MA and ChDHCit:MA) at various temperatures (25, 35, 45, 55, and 65°C). 10 mL of each DES were placed in the test tubes. The test tubes were immersed in the prepared water bath, and a thermometer was used to double-check the temperature. Then, each type of spindle (S61, S62, S63, and S64) was tested to check its suitability for DES liquids. The chosen spindles rotated and a viscosity value appeared on the viscometer display. Measurements were carried out by altering the temperature for 2 min and applying revolutions (50 rpm). The viscosity of the DES was determined and sample testing was performed thrice [23].

Density Measurement

DES was added to a volumetric flask of 10 mL until the calibration mark was reached. An analytical balance was used to weigh the DES (m) in a volumetric flask at 25°C, and the density (d) in g/mL was computed using Equation (1):

$$d \text{ (g/mL)} = m/v \quad (1)$$

in which m denotes the mass (g) of the DES whereas v refers to the DES volume (mL) [17].

Surface Tension Measurement

A force tensiometer (Sigma 700, Attension, Sweden) was employed to measure the surface tension of the eutectic mixtures of ChCl:MA and ChDHCit:MA. The Wilhelmy plate was cleaned by exposing it to a flame before each measurement. The Attension sigma software with an automatic control collected and recorded the surface tension in triplicate at 25°C.

Ionic Conductivity Measurement

The ionic conductivities of ChCl-MA and ChDHCit-MA were determined using a conductivity meter (Hanna Instruments, USA). The conductivity meter was calibrated at 25°C, and measurements were performed after at least 10 min to reach a good temperature equilibrium. To prevent inaccurate readings, the electrode was carefully positioned to avoid contact with the beaker bottom. The ionic conductivity was measured in triplicate and the average value was calculated [24]. Subsequently, the electrode was cleaned with distilled water and dried using clean tissue.

Solubility Tests

A solubility test was performed to check the miscibility of the DES (ChCl:MA and ChDHCit:MA) with solvents of various polarities. 3 mL of DES was placed in 10 mL of test tubes and the level was marked immediately. Seven types of solvents with different polarities, including water, acetic acid, ethanol, methanol, diethyl ether, toluene, and hexane, were tested for their miscibility with DES. The mixture was stirred uniformly for 1 min at 25°C. The occurrence of a clear layer at the specified mark indicates that the added solvent is not miscible with the DES. A layer that forms above the highlighted level indicates that the DES and organic solvent are partially miscible, whereas the absence of a layer indicates that the solvent and DES are miscible [17].

Statistical Analysis

An average of three replicate values for the analyses was obtained for each sample, and one-way analysis of variance (ANOVA) was applied in each experimental phase. Significant differences between treatments at 95% confidence intervals were analysed via Duncan's multiple range test.

RESULT AND DISCUSSION



Visual Characterisation

Table 1 lists the appearance of the prepared DESs. Both DES were in a clear liquid state and exhibited

stability, as both DES remained in liquid form after being left undisturbed for a duration of 24 h. Visual analysis was utilized to determine the homogeneity as well as presence of crystals in the DES liquid [19]. **Figure 1** shows the POM images that confirm that neither DES contained crystals nor residues. This result supports the successful formation of DES. Visually, ChDHCit:MA appeared to be more viscous than ChCl:MA because of the difficulty in transferring the liquid, which required heating for a few minutes. According to Silva et al. [25], citric acid-to-lauric acid-based DES with a mole ratio of 2:1 appeared as a transparent

liquid at room temperature. In contrast, Shumilin et al. [26] found that ChCl-urea in a mole ratio of 1:2 did not form a liquid phase and instead resulted in precipitate formation, indicating instability and unsuitability of this formulation. A comparable observation was noted by Turiel et al. [27], where ChCl-hexanoic acid at a mole ratio of 1:2 showed incompatibility, which leads to precipitate formation. Consequently, the DES formation, even with the same mole ratio of 1:2, does not consistently produce the desired liquid state, as it is substantially impacted by the compatibility between the selected HBA as well as HBD.

Table 1. The appearance of DES with distinct HBAs.

DESs (Moles Ratio)	Visual	Observation	
		After heating	After 24 h
ChCl:MA (1:2)		Liquid	Liquid
ChDHCit:MA (1:2)		Liquid	Liquid

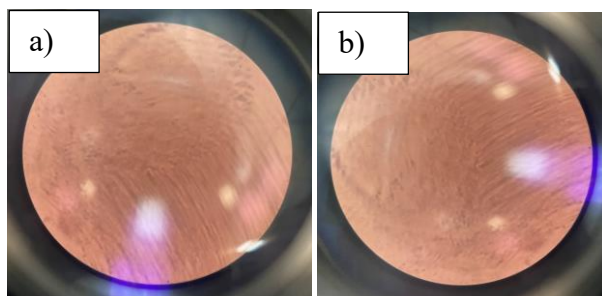


Figure 1. POM images of a) ChCl:MA and b) ChDHCit:MA at total magnification of 10x.

Structural Analysis

FTIR analysis was employed to analyse the functional groups within the chemical structures with the aid of infrared light to observe the bonds and interactions between molecules [18, 25, 28]. The comparison of FTIR peaks of both types of DES with their respective HBA and HBD is presented in **Table 2**. Moreover, the spectrum of pure ChCl showed a wide range of O-H stretching, ranging from 3591.92 to 3228.28 cm^{-1} , in addition to a C-H stretching peak at 2996.00 cm^{-1} . Pure ChCl also exhibited peaks corresponding to C-O and C-N stretching at 1139.94 cm^{-1} and 1083.40 cm^{-1} accordingly, as well as CH_2 and CH_3 bending observed at 1480.14 cm^{-1} , and 1349.14 cm^{-1} . In the meantime, the FTIR spectra of pure ChDHCit showed a broad range of O-H stretching, which ranges from 3597.92 to 2575.03 cm^{-1} , with a C-H stretching peak at 2931.50 cm^{-1} . Pure ChDHCit also displayed peaks indicating C=O, C-O, and C-N stretching at 1708.37, 1228.89, and 1122.60 cm^{-1} , respectively, along with CH_2 and CH_3 bending at 1478.35 and 1369.43 cm^{-1} . Here, the occurrence of C-N stretching in both pure ChCl (1083.40 cm^{-1}) and ChDHCit (1122.66 cm^{-1}) proved that they are quaternary ammonium salts.

In pure ChCl, the wavenumber peaks indicating O-H and C-H stretches overlapped due to possible intramolecular hydrogen bonding between the O-H group in choline cation and chloride anion (1 O-H \cdots Cl $^-$). In contrast, in pure ChDHCit, the possible hydrogen bonding involved four O-H groups (one from choline cation and three from dihydrogen citrate anion) (4 O-H \cdots C₆H₅O₇ $^-$). Consequently, the extent of the O-H stretching varied between the two HBAs. The extent of the O-H stretching was assessed by measuring the difference across the O-H stretching

range, from the highest to the lowest wavenumber. The variation in the O-H stretching range in pure ChDHCit (1022.89 cm^{-1}) was greater than that in pure ChCl (363.64 cm^{-1}). This suggests that the O-H stretching in pure ChDHCit is broader than in pure ChCl. According to Mulia et al. [29], a broader O-H stretching band within a chemical structure indicates a greater number of hydrogen bonds. Therefore, it can be concluded that pure ChDHCit exhibits more hydrogen bonding than pure ChCl.

In the MA spectrum, stretching bands for O-H, C-H, C=O, and C-O were observed within the range of 3403.84 to 2581.13 cm^{-1} , at 2908.25 cm^{-1} , 1706.49 cm^{-1} , and 1166.31 cm^{-1} , respectively. Additionally, MA exhibited a CH_2 bending at 1549.13 cm^{-1} , while no wavenumber peaks were observed for CH_3 bending and C-N stretching. The presence of the stretches of C=O and O-H proved that MA is a dicarboxylic acid [30]. In MA, the overlapping of O-H and C-H stretches can be linked to the potential occurrence of dimerization through intramolecular hydrogen bonding between hydrogen atoms from one carboxyl group (COOH) and the oxygen atom of another COOH group within its molecular structure. In the spectrum of MA, the disparity in the wavenumber range of O-H stretching, starting from the highest to the lowest, was approximately 822.71 cm^{-1} , indicating a broader range compared to pure ChCl (363.64 cm^{-1}).

Structural changes in DES, ChCl:MA, and ChDHCit:MA were observed by comparing the spectrum to the individual components in DES, as illustrated in **Figure 2**. New interactions, such as ionic bonds and hydrogen bonding, as illustrated in **Figure 3**, are responsible for the shifts in the FTIR peaks.

Table 2. Peaks and wavenumber exhibited by each DES.

	Wavenumber (cm^{-1})						
	O-H stretch	C-H stretch	C=O stretch	CH_2 bend	CH_3 bend	C-O stretch	C-N stretch
ChCl	3591.92-3228.28	2996.00	ND	1480.14	1349.14	1139.94	1083.40
MA	3403.84-2581.13	2908.25	1706.49	1549.13	ND	1166.31	ND
ChDHCit	3597.92-2575.03	2931.50	1708.37	1478.35	1369.43	1228.89	1122.60
ChCl:MA (1:2)	3538.16-2553.79	2934.29	1714.64	1478.77	1378.99	1152.32	1082.73
ChDHCit:MA (1:2)	3552.23-2557.35	2961.59	1711.76	1572.24	1374.47	1190.25	950.36

ND = Not detected.

Note: ChCl was Choline Chloride, ChDHCit was Choline Dihydrogen Citrate and MA, malonic acid.

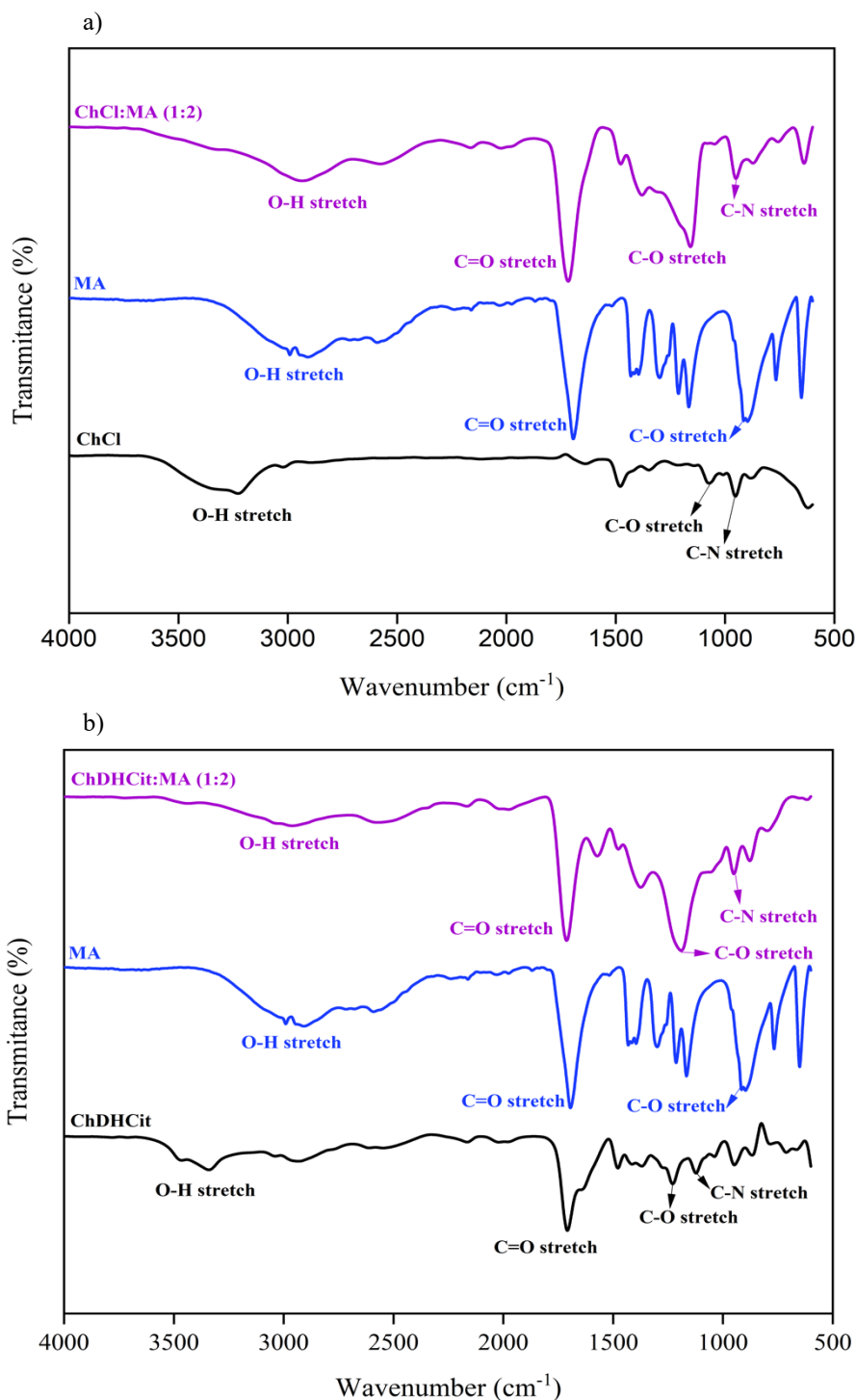


Figure 2. FTIR spectra of a) ChCl, MA, ChCl:MA (1:2) and b) ChDHCit, MA, ChDHCit:MA (1:2).

These anions were positioned at the centre and bridged the interaction between choline and malonic acid. The O-H groups on MA were attracted to the Cl⁻ and C₆H₅O₇⁻ anions, producing O-H ··· Cl⁻ and O-H ··· C₆H₅O₇⁻ bonds, accordingly. This bonding affects the wavenumber values in C-O stretching within MA, which appeared to decrease from 1166.31 to 1152.32 cm⁻¹ in ChCl:MA after bonding with the chloride anion. Surprisingly, the C-O stretching in MA increased to 1190.25 cm⁻¹ in ChDHCit:MA after successful bonding

with the dihydrogen citrate anion, which implies that C-O in MA is more polarised owing to the high electron density and the larger size of the electron cloud. The C-O peak in ChDHCit:MA is also more intense than its component, possibly due to a higher degree of hydrogen bonding in ChDHCit, leading to an increased dipole moment of the C-O bond. Nevertheless, the wavenumber of C=O stretching in both DES showed a slight increase in comparison with the wavenumber peak for MA owing to the location of C=O which

is far higher than that of C-O. The C-N peak in ChDHCit:MA also shifted to a lower wavenumber (950.36 cm^{-1}) compared to the C-N peak in pure ChDHCit (1122.6 cm^{-1}). The hydrogen bonds existence in the DES system was validated by Gautam et al. [31]. They effectively assessed the ChCl: acetic acid-based DES and ChCl: formic acid-based DES using FTIR, Quantum Theory of Atoms in Molecules (QTAIM), and Reduced Density Gradient (RDG) analyses due to the accurate topology of the gradient vector field. In our study, the disparity in the wavenumber range of O-H stretching within ChDHCit:MA, from the highest to the lowest, was approximately 994.88 cm^{-1} , higher than that of ChCl: MA (984.37 cm^{-1}). Therefore, ChDHCit:MA is suggested to have a more hydrogen bonding than ChCl:MA.

The various HBAs displayed subtle variations in their FTIR spectra with noticeable discrepancies between the observed peaks of ChCl:MA and ChDHCit:MA. The wavenumber peaks indicating the stretching of O-H, C-H, C-O, and bending of CH_2 shifted upward from 2953.00 to 2988.00 cm^{-1} , 2934.29 to 2961.59 cm^{-1} , 1152.32 to 1190.25 cm^{-1} , and 1478.77 to 1572.24 cm^{-1} , respectively. In contrast, the wavenumber peaks of C=O, C-N stretching, and CH_3 bending shifted downward from 1714.64 to 1711.76 cm^{-1} , 1082.73 to 950.36 cm^{-1} , 1378.99 to 1374.47 cm^{-1} . This is because ChDHCit changes the bond strength more effectively than ChCl because of its more complex structure with more O-H groups. The complex structure of $\text{C}_6\text{H}_5\text{O}_7^-$ in ChDHCit:MA induced more spectral changes in FTIR spectra than Cl^- in ChCl:MA. This occurred because of the changes in electron density during the formation of hydrogen bonds within both DES systems, which led to changes in the frequency of the stretching vibration. Thus, the hydrogen bonding strength was strongly dependent on the chosen HBA. The more extensive the structure

with O-H and COOH groups, the more hydrogen bonding occurs, resulting in a wider O-H stretching and higher shift in the wavenumber observed in the FTIR spectra [32].

Thermal Stability

Thermogravimetric analysis (TGA) was utilised to examine the thermal stabilities of the solid, liquid, and mixed samples. This technique involves measuring the weight loss as it is heated at a controlled rate [33,34]. In this study, solid ChCl, ChDHCit, MA, liquid ChCl:MA, and ChDHCit:MA were analysed and compared to determine their decomposition temperatures (T_d). The intersection points between the baseline weight as well as the tangent of the weight versus temperature curve was plotted, as shown in **Figure 4**, to identify the initial degradation step of the process for each sample. As seen in **Figure 4(a)** as well as **Figure 4(b)**, a small weight loss of 3.78% in ChCl and 3.04% in ChDHCit at temperatures below 100°C is generally due to water evaporation from its hygroscopic nature [33]. ChCl participated in one degradation step, which was the dissociation of the ionic link between the Cl^- anion and the Ch^+ cation which occurred around 300.16 to 363.92°C with a weight loss of approximately 96.22%. However, ChDHCit required two stages of degradation, as shown in **Figure 4(b)**, in which the first weight loss at 79.02% dissociated the ionic bonds between the $\text{C}_6\text{H}_5\text{O}_7^-$ anion and Ch^+ cation from 160.46 to 260.89°C which is much lower than that in ChCl. The second stage of disruption involved hydrogen bonding within the $\text{C}_6\text{H}_5\text{O}_7^-$ anion, from 260.89 to 488.53°C , with a much smaller weight loss of 13.49%. Hence, although ChDHCit is less thermally stable compared to ChCl, it fully degrades (100%) at higher temperatures of 557.72°C , because more bonding to be disrupted in the molecule.

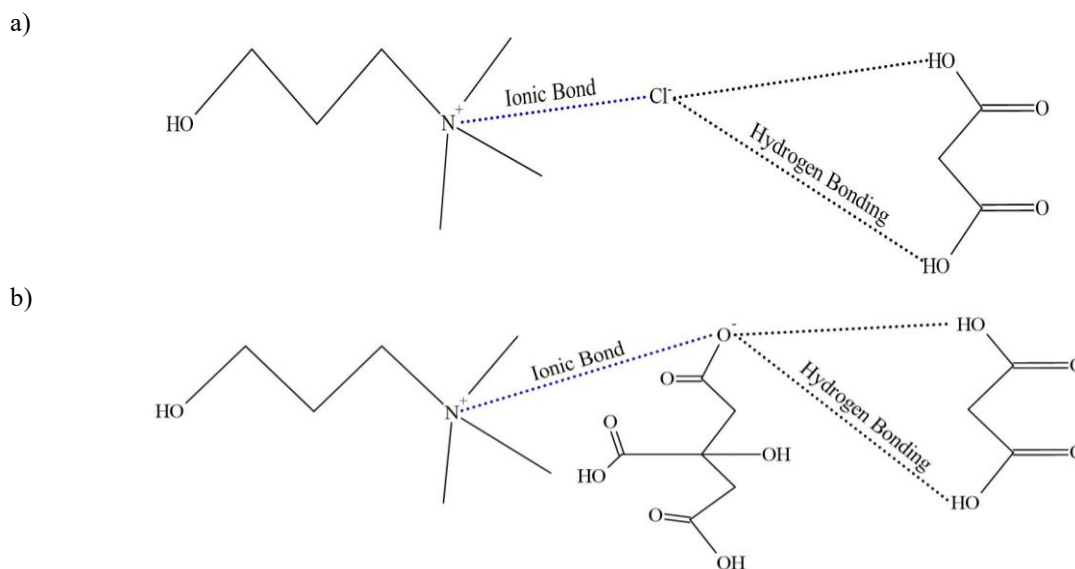


Figure 3. Formation of hydrogen bonds between a) ChCl and MA and b) ChDHCit and MA.

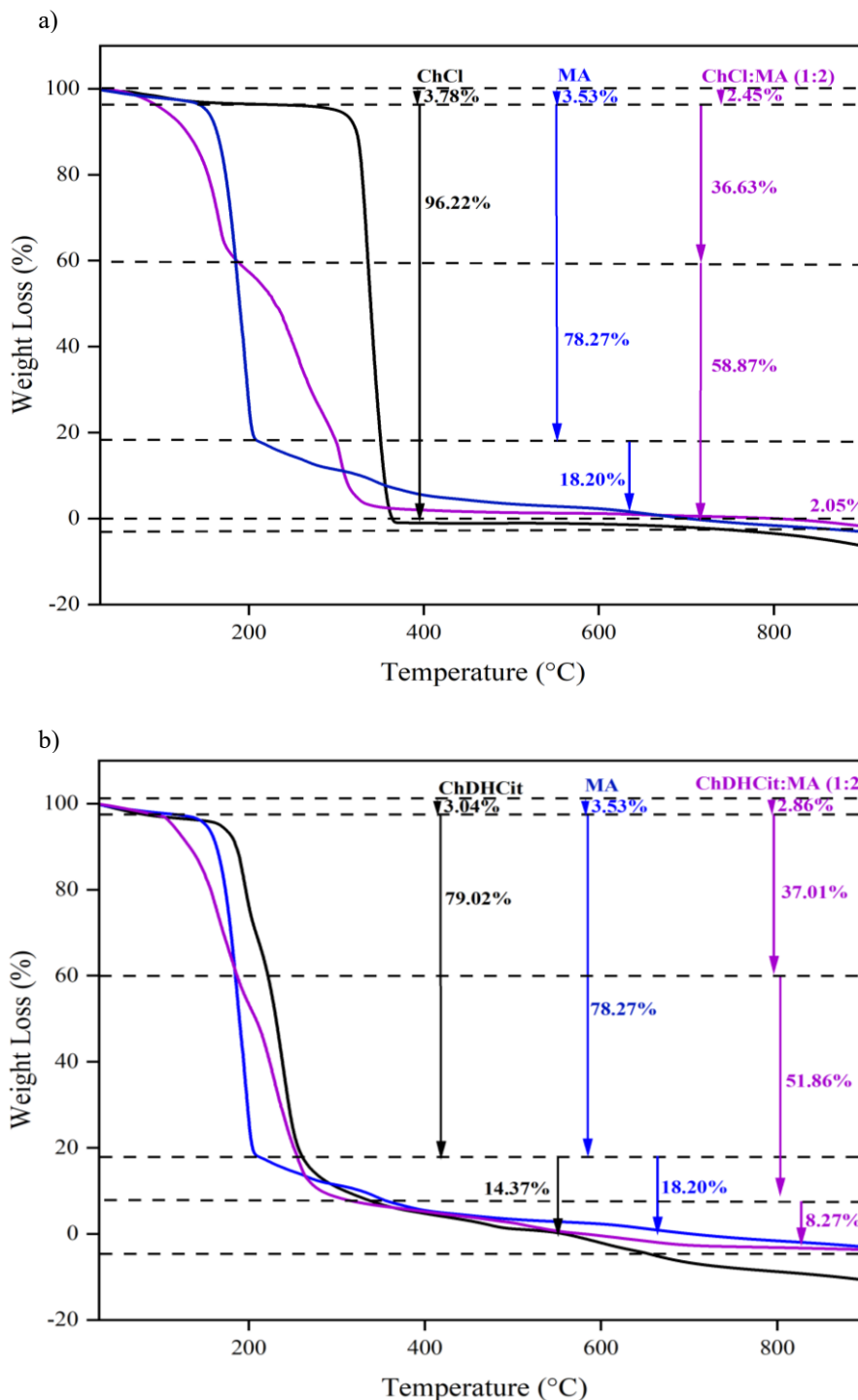


Figure 4. Weight loss of a) ChCl, MA, ChCl:MA and b) ChDHCit, MA, ChDHCit:MA at 30-900°C.

The degradation of MA started with the loss of water molecules from 30.14 to 99.85°C, decarboxylation of MA into acetic acid from 99.85°C to 210.07°C with a percentage weight loss of 78.27%, and further decomposition to carbon dioxide as the final product with 18.20% loss. Meanwhile, the thermal degradation of the eutectic mixtures ChCl:MA and ChDHCit:MA occurred in multiple stages: the loss of hydrogen bonding and the decomposition of DES into smaller molecules.

The degradation curve in DES was not smooth, indicating the decomposition of HBA and HBD in the DES network. For both DES, the water that being absorbed during DES preparation started to evaporate up to 81.86°C with 2.45% for ChCl:MA and 99.94°C with 2.86% for ChDHCit:MA. Continual heating from 81.86 to 180.48°C (**Figure 4a**) caused the ChCl:MA to dissociate the hydrogen bonding from MA, which then led to the removal of MA into smaller molecules such as CO₂ with 36.63% weight loss,

followed by dissociation of the Ch^+ cation and Cl^- anion from 180.48 to 330.56°C with 58.87% weight loss. After 330.56°C, the remaining 2.05%, $\text{ChCl}:\text{MA}$ slowly decomposed into other small molecules up to 700°C. In $\text{ChDHCit}:\text{MA}$ (Figure 4b), the degradation point indicating the breakdown of hydrogen bonding between ChDHCit and MA clearly happened between 99.94°C 186.60°C with a percentage weight loss

of 37.01%. Due to the structural complexity of ChDHCit , the self-disruption of hydrogen bonding within ChDHCit was degraded from 186.60 to 580°C with a percentage weight loss of 51.86% in the following stages. This suggests that ChCl and ChDHCit have strong affinities for MA for the formation of DESs, which required extra heating to disrupt the bonding in eutectic mixture.

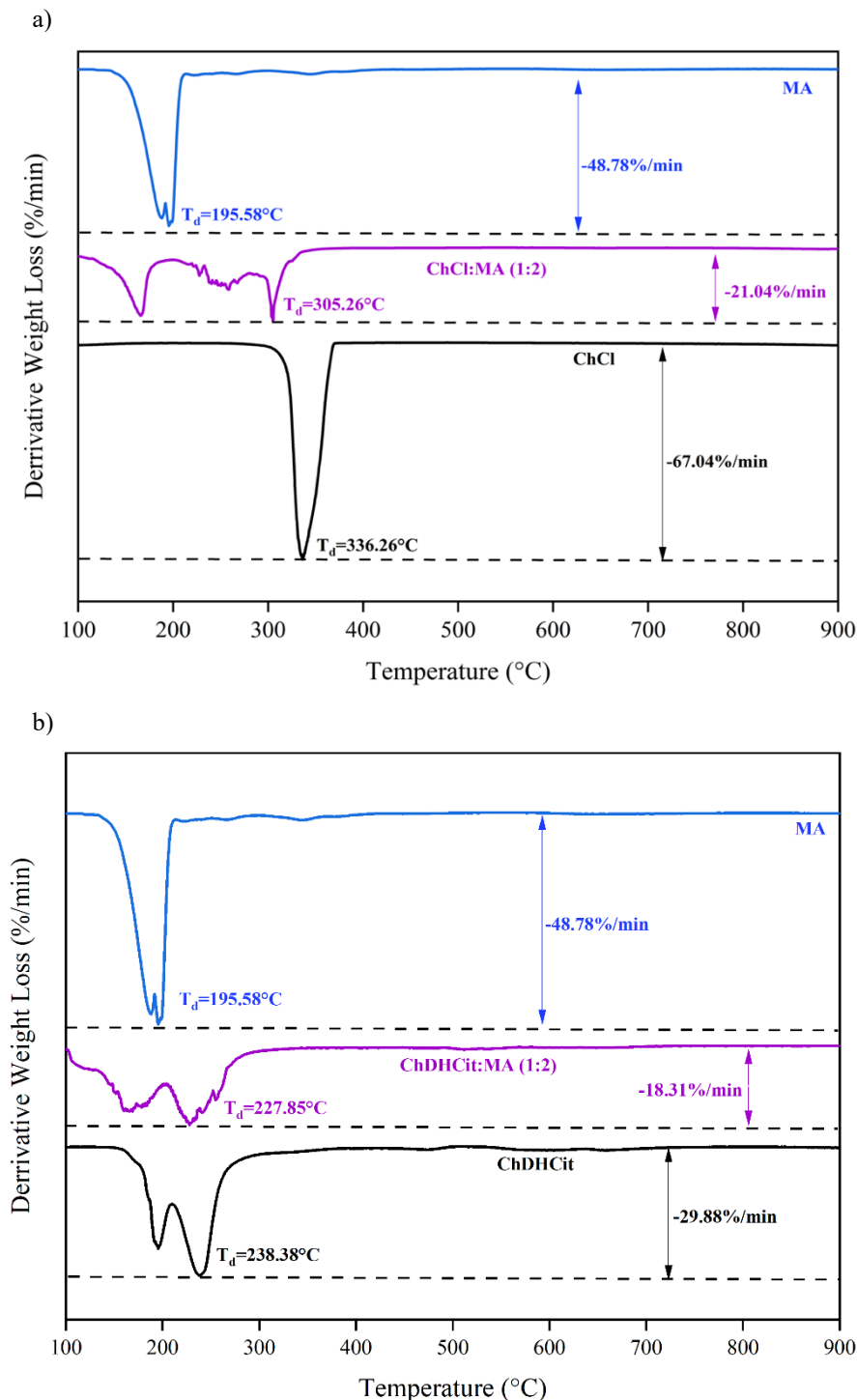


Figure 5. Derivative weights of a) ChCl , MA , $\text{ChCl}:\text{MA}$ and b) ChDHCit , MA , $\text{ChDHCit}:\text{MA}$ at 30-900°C.

The inflection point in **Figure 4** can be obtained from a dm/dT curve to estimate the characteristic temperatures of the degradation process at its maximum, referred to as T_d . Hence, a graph of the derivative weight loss (DTG) versus temperature was plotted, as shown in **Figure 5**, to confirm the T_d values, where the peaks correspond to the different stages and the maximum rate of thermal degradation. Overall, the acquired T_d values matched the deterioration range, as shown in **Figure 4**. As depicted in **Figure 5**, both DES demonstrated the presence of two peaks, which are associated with the T_d peak of MA and the T_d peak of HBAs (ChCl, ChDHCit). The T_d of DES was identified at the highest derivative weight loss, which suggests that the T_d of ChCl:MA and ChDHCit:MA were 305.26°C and 227.85°C, respectively.

The addition of MA with a lower T_d value (195.58°C) into HBA reduced the T_d value of DES, which demonstrated the hydrogen bonds formation in DES. This showed the existence of interactions in the DES, not only mechanical mixing. The T_d values of DES are influenced by the size of the anion in HBA. In the case of ChDHCit:MA, the larger dihydrogen citrate ($C_6H_5O_7^-$) anions may not form stable hydrogen bonding networks due to steric hindrance, resulting in lower overall thermal stability. Steric hindrance refers to the obstruction of strong hydrogen bonds that exists between the oxygen anion in asymmetrical DHCit and the hydrogen in MA. On the other hand, the chloride (Cl⁻) anions in ChCl:MA, being smaller and more symmetrical, allow for better interaction with MA, leading to a more stable and thermally resistant DES. This explains why the T_d of ChCl:MA (305.26°C) is higher than that of ChDHCit:MA (227.85°C). Therefore, the strength of hydrogen bonding is not solely dependent on the number of hydrogen bonding sites available, but also on the possible steric hindrance that can affect the overall thermal stability of the DES. These results agree with those of a study by Gajardo-Parra et al. [35], who studied the T_d values of ChCl-based DESs with HBDs of different sizes (levulinic acid, ethylene glycol, and phenol). They reported that the T_d values of ChCl-LA, ChCl-EG, and ChCl-phenol were 244.72, 264.86 and 240.23°C. Hence, in this study, the greater T_d value of ChCl:MA indicated a thermally stable DES compared to ChDHCit:MA.

The expected behaviour of DES is that the T_d value falls between the T_d values of its respective HBA and HBD. However, a deviation was observed for ChCl:MA and ChDHCit:MA owing to the thermal sensitivity of MA. An identical pattern was reported by Delgado-Mellado et al. [36], who discovered that the T_d values of ChCl:MA, ChCl, and MA were 99.85, 270.55, and 134.85°C, respectively. MA in the ChCl:MA starts to decompose at 166.01°C whereas in the ChDHCit:MA at 166.23°C, which were lower than the T_d of pure MA (195.58°C), respectively. This early decomposition is due to the interaction between

the HBAs (ChCl and ChDHCit) with MA, which alters the thermal stability of their respective DES systems. This is because MA undergoes significant changes to acetic acid, which makes the DES less thermally stable. The generation of acetic acid lowers the pH of the DES, leading to an increase in the decomposition rate constant [37,38,39]. By means, the first breakdown of the DES components started at lower temperature correspond to the decomposition of its HBD and then its HBA components at later higher temperature.

Both ChCl:MA and ChDHCit:MA are associated for use in many high-temperature applications such as extraction and separation processes, reaction media in organic reactions, electrolytes in electrochemical devices, and solvents for polymer dissolution [40-44]. The extensive hydrogen and ionic bonds within ChCl:MA and ChDHCit:MA resulted in strong steric hindrance and led to thermal stability. Therefore, additional energy is necessary to disrupt and weaken the bonds. The larger the anion with more binding sites in the DES (ChDHCit), the stronger the interaction in the DES. This demonstrates that HBA or anions play a crucial role in producing DES that are less vulnerable to thermal deterioration. A prior investigation by Majid et al. [45] emphasized the impact of HBD on tetrabutylammonium chloride (TBAC)-based DES utilizing ethylene glycol, tetraethylene glycol, and polyethylene glycol as various HBD. According to them, the order of thermal stability was observed as TBAC-EG < TBAC-TEG < TBAC-PEG with T_d of 222.13, 259.21, 378.15°C, respectively. HBDs with low boiling points are easily degraded and damaged [46, 47]. Furthermore, they noted that extending the alkyl chain length of the HBD yield a greater amount of heat needed to overcome the intermolecular forces occurred in the DES eutectic mixture. Overall, it can be concluded that both HBA and HBD affected the thermal stability of the prepared DES.

The implications of differences in thermal stability among DES are significant across various practical applications, including biomass processing, protein stabilisation, and extraction processes. In biomass processing, DESs are employed in the fractionation and dissolution of biomass components, such as lignin and cellulose. The high thermal stability of DES is crucial in these applications to prevent decomposition at elevated temperatures. For instance, DESs composed of ChCl with various HBDs like oxalic acid dihydrate and glycerol exhibit non-linear weight loss at temperatures exceeding 80°C, indicating that biomass processing should ideally occur below this threshold to preserve solvent integrity [48]. In the context of protein stabilisation, the high thermal stability of DESs can enhance the stability of proteins. For example, Pal et al. [49] compared the efficacy of ChCl-glycerol as a DES with that of a water medium in maintaining the stability of Trp-cage mini protein in glycylglycine. They discovered that the protein was denatured from its native state in the water medium at 126.85°C, whereas it maintained its native

conformation in the DES medium. This application of DES renders them suitable for biocatalytic reactions and the long-term storage of biomolecules. In pectin extraction, DESs present significant advantages over strong acids, which are the conventional solvents for this process. DESs are characterised by their high thermal stability, lower corrosiveness, and safety for use, leading to enhanced extraction efficiency and improved functional properties. For instance, Lin et al. [50] found that pectin extracted from grapefruit peel using betaine-citric acid yielded 36.47%, a markedly higher yield compared to the 8.76% pectin yield obtained with hydrochloric acid under a solid-to-liquid ratio of 1:25 g/mL, a pH of 2, a temperature of 85°C,

and an extraction time of 120 minutes. Furthermore, they noted that pectin extracted using betaine-citric acid exhibited a higher value of rhamnogalacturonan-I, more arabinan side chains, and a higher molecular weight, when compared to pectin extracted using hydrochloric acid. Consequently, pectin extracted using DES demonstrated superior emulsifying activity and stability compared to hydrochloric acid-extracted pectins, suggesting its potential as an emulsifier in the food industry. Thus, the high thermal stability of DES, combined with their eco-friendly characteristics and high extraction efficiency, positions them as an excellent alternative to traditional organic solvents across various applications.

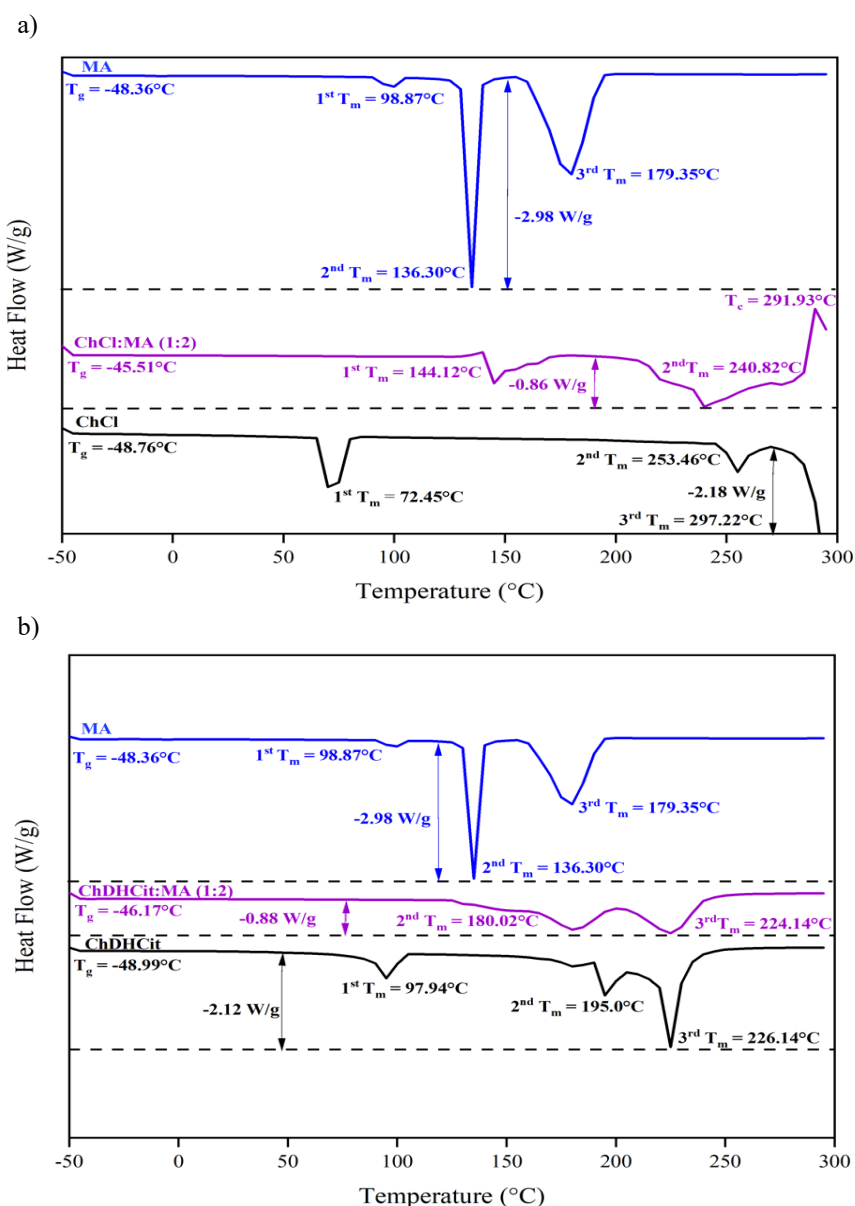


Figure 6. Heat flow of a) ChCl, MA, ChCl:MA and b) ChDHCit, MA, ChDHCit:MA at -50-300°C.

Table 3. T_m , T_g , and T_c of each DES.

	T_m (°C)	T_g (°C)	T_c (°C)
ChCl	297.22	-48.76	-
ChDHCit	97.94	-48.99	-
MA	136.30	-48.36	-
ChCl:MA (1:2)	144.12	-45.51	291.93
ChDHCit:MA (1:2)	180.02	-46.17	-

Melting, Glass Transition, Crystallisation Temperature

Differential scanning calorimetry (DSC) was utilized to assess the melting points of solid, liquid, and mixed samples. The idea is to measure the heat flow related to the thermal events happening in the sample in relation to temperature changes. Generally, melting point (T_m) resembles the temperature at which the solid phase transitions to the liquid phase [41]. The eutectic point of a DES is known as its eutectic temperature or the minimum T_m value [14]. This technique was used to determine the T_m of solid ChCl, ChDHCit, MA, liquid ChCl:MA, and ChDHCit:MA by observing endothermic peaks in the DSC curves, as displayed in **Figure 6**. Here, the peaks corresponding to the T_m of ChCl, ChDHCit, MA, ChCl:MA, and ChDHCit:MA are 297.22, 97.94, 136.30, 144.12, and 180.02°C, respectively. This proves that both DES reached their eutectic points, indicating that solid ChCl, ChDHCit, and MA successfully melted into liquid ChCl:MA and ChDHCit:MA.

Table 3 presents a summary of the melting point (T_m), glass transition (T_g), and crystallisation temperature (T_c) for each component. The T_g of DES refers to a phase transition phenomenon from a more ordered or glassy state to a more mobile and less viscous state. DES are generally characterised as mixtures with low T_g values [47]. As displayed in **Figure 6**, the T_g values of ChCl:MA and ChDHCit:MA were -45.51, -46.17°C, accordingly, meanwhile the T_g values of pure ChCl, ChDHCit, and MA were -48.76, -48.99, and -48.36°C, respectively. The higher T_g value of DES compared to the T_g of its constituent indicated stronger hydrogen bonding in DES, as more heat was needed to absorb in order to overcome these interactions. According to Hammond et al. [51], these hydrogen-bonding interactions are primarily responsible for the less-ordered and non-rigid molecular arrangement within the DES system, allowing for their flexibility and adaptability. Therefore, it can be said that the liquid starts to move more freely after passing the T_g . In addition, the crystallisation temperature (T_c) was observed only for the phase transition of ChCl:MA at 291.93°C. T_c indicates that ChCl:MA solidifies at the reported temperature. Therefore, to preserve its liquid state, ChCl:MA should be used below the reported temperature.

The T_m of DES is influenced by lattice energy and interactions between its components. Notably, ChCl:MA obeyed the general rule of eutectic formation of DES, in which the T_m value (144.12°C) was between that of its constituents (T_m MA = 136.30°C, T_m ChCl = 297.22°C). This agrees with Sai et al. [20], who proved that the T_m value of a hydrophobic DES was 9°C which was also between the T_m values of its components, thymol and tetradecanol. Pure ChCl exhibited a comparably elevated lattice energy, thereby necessitating a larger amount of energy to disrupt its crystal lattice. Nonetheless, due to the straightforward and small structure of the chloride anion (Cl^-) in ChCl, when it interacts with hydrogen in MA, it facilitates efficient hydrogen bonding and charge delocalisation. This interaction leads to the dispersal of the charge over a broader region, thereby diminishing the overall electrostatic attraction and resulting in a lowered T_m of ChCl:MA DES to 144.12°C.

Surprisingly, there was an exception for ChDHCit:MA, as the T_m value (180.02°C) was reported to be higher than that of its constituents (T_m MA = 136.30°C, T_m ChDHCit = 97.94°C). This phenomenon can be justified by the increased quantity of hydroxyl and carboxylic groups found in the structure of ChDHCit. These functional groups contribute to an increased likelihood of forming hydrogen bonds with MA, thereby necessitating a greater amount of energy to disrupt these interactions. However, it should be noted that the robust hydrogen bonding network alone is not the sole determining factor [52, 53]. Rather, the substantial and non-symmetrical size of DHCit anion ($C_6H_5O_7^-$) plays a critical role, as it can potentially cause steric hindrance that counteracts and diminishes the effects of the strong hydrogen bonding, ultimately resulting in a higher T_m of the ChDHCit:MA DES to 180.02°C.

Hence, the effects of different HBAs in the DES system suggested that ChDHCit:MA had a higher T_m than ChCl:MA. Similar findings were mentioned by AlOmar et al. [54], who conducted a study on a glycerol (Gly)-based DES paired with various hydrogen bond acceptors (HBAs), including benzyl-triphenyl-phosphonium chloride (BTPC), methyl-triphenyl-phosphonium bromide (MTPB), ChCl, triphenyl phosphonium bromide (ATPB), diethyl ethanol-ammonium chloride (DAC), and tetrabutylammonium

bromide (TBAB). The researchers discovered that BTPC-Gly exhibited the highest T_m value of -21.99°C , while ChCl-Gly exhibited the lowest T_m value of -33.47°C . According to their findings, an increase in the size of the HBA led to a more compact arrangement of molecules and weaker intermolecular forces, resulting in a higher melting point, and vice versa. Silva et al. [25] stated that capric acid based DESs exhibit different T_m values because of the different chain lengths of the HBDs. They reported that combination of capric acid as HBA with stearic acid as the longest HBD at a mole ratio of 4:1 had the highest T_m value of 28.80°C . Thus, choosing HBA and HBD is crucial for determining the T_m value of DES.

Acidity

Acidity refers to the quality, state, degree of sourness, and tartness of the substance. It can be quantified by the quantity of acid in a substance or solution. In a chemical sense, acidity is typically associated with the concentration of hydrogen ions (H^+) in the solution. In this research, a digital pH meter was utilized to assess and contrast the acidities of liquid ChCl:MA and ChDHCit:MA to assess the effects of different HBA on the DES acidity, as shown in **Figure 7**. The acidic nature of MA as an HBD is expected to result in a low pH for both the DES. The results suggest that ChCl:MA had a lower pH (1.19 ± 0.05^a) than ChDHCit:MA (4.24 ± 0.01^a).

The interaction and behavior of HBA and MA in a solvent system can greatly affect the acidity and stability of the solution. The acidity of DES is affected by the acidic characteristics of MA, particularly its capacity to donate protons. Malonic acid, which is a weak diprotic acid, can donate two hydrogens, leading to the release of H^+ cations into the solution and the formation of a malonate anion (the conjugate base) [55]. As a result, the system's pH was impacted by H^+ cations concentration and the acid's strength. The stability of the malonate ion (the conjugate base) was essential for determining the solution's overall acidity. A stable conjugate base affects the acidity of the DES. Highly stable malonates are less likely to readily accept a proton from the solution (H^+), increasing the H^+ concentration, thereby increasing the acidity of the DES [56]. In this case, the malonate anions might be stabilised by the interaction of the negatively charged oxygen atoms on the malonate anion ($\text{CH}_2(\text{COO}^-)_2$) with the positively charged ammonium group and hydroxyl group in the choline cation $[(\text{CH}_3)_3\text{NCH}_2\text{CH}_2\text{OH}]^+$ through electrostatic interactions and hydrogen bonding, respectively. The interaction of malonate anions with these two possible sites in choline is more stable in ChCl:MA than in ChDHCit:MA, which leads to the DES ChCl:MA being more acidic than ChDHCit:MA. The bulky group of the $\text{C}_6\text{H}_5\text{O}_7^-$ anion could cause steric hindrance and affect the accessibility of the malonate ions to these sites, leading to less acidic ChDHCit:MA.

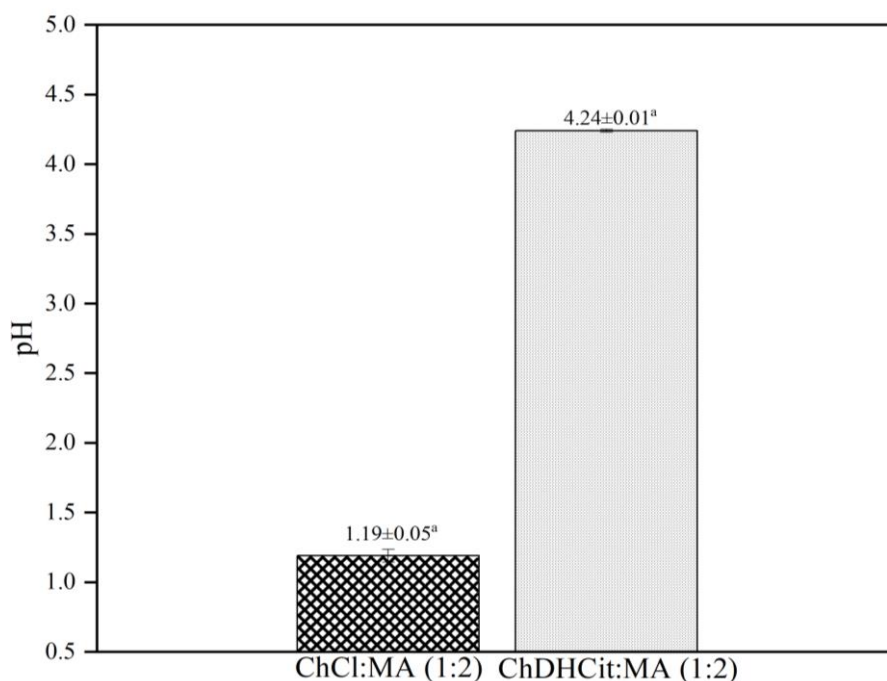


Figure 7. pH of the ChCl:MA and ChDHCit:MA mixtures at 25°C .

Modifying the HBA in the DES formulation can greatly affect the final pH of the prepared DES, since the interaction between the HBA as well as HBD impacts the overall acidity and basicity of the DES. Previously, Fuad et al. [57] categorised the DES into acidic, sugar, and alcohol-HBD-based DES and found the DES were in the pH range of 2.53 ± 0.02 - 4.42 ± 0.07 , 6.44 ± 0.13 - 6.64 ± 0.38 , and 5.95 ± 0.19 - 8.53 ± 0.14 , respectively. This demonstrates that the pH of DES can vary depending on the chosen HBA or HBD. Teles et al. [58] evaluated the acidity of DES created from ammonium-based salts and carboxylic acids by employing solvatochromic parameters, referred to as hydrogen bond acidity (α), hydrogen basicity (β) as well as dipolarity/polarizability (π^*). They noted that the carboxylic acid component primarily plays a significant role in the high acidity of the DES. The researchers also observed that the hydrogen bond acidity (α) is highly dependent on the anion of the salt, with chloride-based salts typically exhibiting higher α values compared to bromide-based salts due to stronger cation-to-anion interactions. These strong interactions enhance the proton donation ability of the HBD when it interacts with the HBA, thereby stabilising the DES structure. Consequently, the lower pH value of ChCl:MA (1.19 ± 0.05^a) in comparison to ChDHCit:MA (4.24 ± 0.01^a) can be linked to the higher hydrogen bond acidity and stronger hydrogen bond interactions of ChCl with MA, respectively. These factors result in greater proton availability in the solution.

Studying the acidity contributes to a better understanding of how each DES acts in certain applications. An acidic DES is appropriate for extraction, for instance, the extraction of pectin from fruit waste, because it allows mild conditions that help preserve the quality of the extracted pectin and improve its yield [59, 60]. This is because the high concentration of H^+ cations from the solvents effectively protonates the carboxylic group of pectin which is deprotonated (COO^-) at neutral or slightly basic pH. Hence, repulsion can be reduced, enabling pectin to dissolve easily in the extraction solution [61,62]. Specifically, these H^+ cations successfully aided the disruption of hydrogen bonding and electrostatic interactions that held pectin molecules in the middle lamella walls. Previously, basic DES, such as ChCl-urea, have been reported as promising protein extractors for sea buckthorn seed meal, without affecting their quality [63]. This is because the high concentration of OH^- ions disrupts the structure of proteins, causing them to unfold and lose their native conformation. This unfolding exposes the hydrophobic regions of the proteins, which can interact with OH^- ions and lead to the formation of protein-hydroxide complexes. This complex was easily separated from the rest of the seed meal, allowing the release of proteins. In conclusion, the design of DES revolves around the strategic selection of HBAs and HBDs to attain the ideal acidity level tailored for a specific purpose.

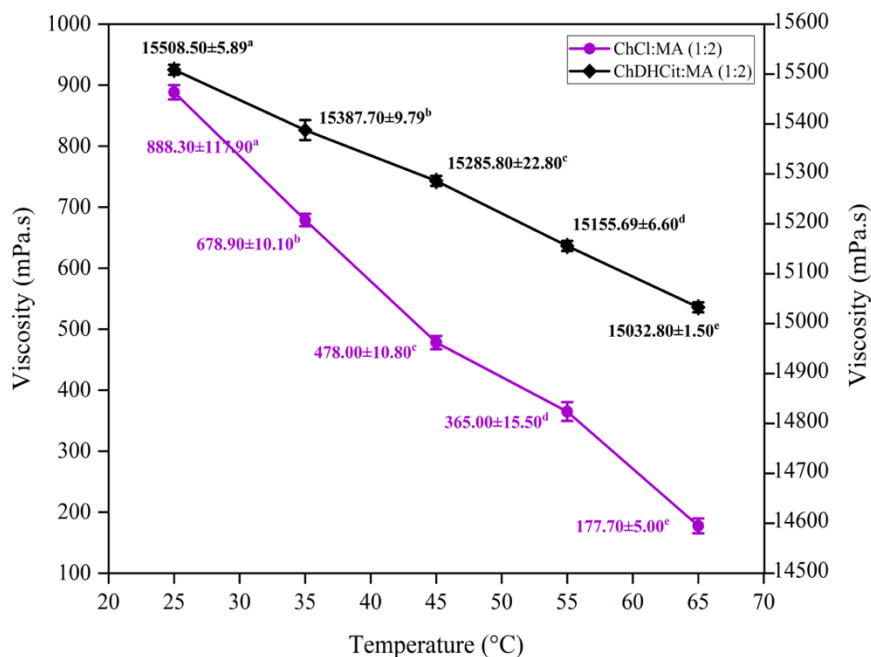


Figure 8. Viscosities of ChCl:MA and ChDHCit:MA at 25°C.

Viscosity

Viscosity denotes the measurement of the resistance of a liquid to flow and deformation. This describes the internal friction within the moving fluid. Liquids with high viscosity flow more slowly, whereas those with low viscosity flow more easily [17]. The viscosity or fluid thickness is influenced by the intermolecular forces of attraction within the liquid. When these forces were strong, the viscosity of the liquid increased. The DES viscosity exceeds that of typical organic solvents and associates with the hydrogen bonding between the HBA and HBD [64-66]. The viscosities of ChCl:MA and ChDHCit:MA from 25 to 65°C are shown in **Figure 8**. These results suggest that ChCl:MA has a viscosity range of 888.30 ± 117.90^a to 177.70 ± 5.00^c mPa·s, which is lower than that of ChDHCit:MA in the range of 15508.50 ± 5.89^a to 15032.80 ± 1.50^c mPa·s. **Figure 8** also shows that the DES viscosity decreases with an increment in temperature. Both DES experienced a decrease in internal resistance, in which the hydrogen-bonding network was disrupted or weakened at high temperatures. According to the theory of mobility of species in DES, heat accelerates molecular movement, resulting in a larger space area, enabling molecular movement. These results reflect those of Lapena et al. [64], as the viscosities of ChCl-ethylene glycol and ChCl-ethylene glycol-water showed the same trend which increasing temperature from 5 to 65°C reduced the viscosity from 100.9 to 10.90 mPa·s, and 66.65 to 7.966 mPa·s, respectively.

The effects of various HBA on the viscosities of the DES were also investigated. As shown in **Figure 8**, the viscosity of ChDHCit:MA was greater than that of ChCl:MA at temperatures that ranges from 25 to 65°C. This is because of the structure of ChDHCit is more complex than that of ChCl. The occurrence of hydroxyl and carboxylic groups in ChDHCit increases the possibility of hydrogen bond formation between molecules, producing a very viscous liquid. This is related to the free volume or holes having appropriate dimensions [67, 68]. Free volume refers to the unoccupied spaces within a material that facilitate molecular movement. It is a critical factor in determining the material's physical properties, such as viscosity and diffusion. The concept of free volume is associated with viscosity; specifically, an increase in free volume within a material enhances the mobility and rearrangement of molecules, resulting in lower viscosity. In this case, the movement of ChDHCit was restricted owing to the large and non-symmetric size of the dihydrogen citrate ions and the more hydrogen bonding with MA. **Figure 8** also known as there is a difference for the viscosities of each DES to be altered or changed by temperature. The larger size and more complex shape of ChDHCit:MA may result in a smaller decrease in viscosity than that of ChCl:MA. This suggests that the presence of a large $C_6H_5O_7^-$ ion

leads to a less flexible DES than that a with smaller Cl^- ion. The flexibility of ChCl:MA enables molecules to be packed more tightly and to flow more smoothly as the temperature increases. Consequently, the viscosity of MA-based DESs may be adjusted by altering the temperature, showcasing their adaptability to fulfil specific application needs.

A study by AlOmar et al. [54] discovered that methyl-triphenyl-phosphate bromide MTPB-glycerol (Gly) with a larger size of HBA was more viscous with a value of 2775.9 cP than ChCl-Gly with a value of 281 cP. In addition, Savi et al. [69] reported that ChCl-citric acid is more viscous compared to ChCl-lactic acid, owing to its extensive hydrogen bonding and high molecular weight. The high and low viscosities of DES exhibit different roles in certain applications. For instance, viscous DES are preferable as active solvents in catalytic reactions because they help increase the contact between the catalyst and the reactants [70]. In contrast, less viscous DES are suitable for gas separation [71], liquid-phase microextraction [72], corrosion protection [73], and as green substitutes for extraction media [74]. The low viscosity value was reported to be approximately 19 cP at room temperature for ChCl-ethylene glycol having a molar ratio of 1:4 which is commonly used in the development of CO_2 -philic separation membranes [75,76]. Moreover, there exists a correlation between viscosity and industrial applications, particularly in extraction processes. For instance, a lower viscosity of DES can enhance the solubility of pectin, thereby facilitating its extraction by allowing pectin molecules to diffuse more readily from plant cell walls into the DES. This improved interaction between the DES and the plant material results in increased extraction efficiency [77]. Thus, choosing the right viscosity is crucial for maximising the performance, energy usage, product quality, equipment compatibility, and even safety in a range of applications.

Density

The density of a liquid is defined by its degree of compactness. This indicates the proximity of the liquid molecules packed together. The DES is a liquid; therefore, its density can be determined by dividing the amount of matter contained in the volume it occupies. In this study, the densities of the two types of DES were measured at 25°C, as shown in **Figure 9**. These results suggest that ChCl:MA was denser than ChDHCit:MA, with values of 1.1464 ± 0.0003^a and 1.0878 ± 0.0002^a g/mL, respectively. These density values agree with those reported in the literature for most DES, in which the density was greater compared to that of water and between 1.00 to 1.35 g/cm³ at 25°C [78, 79]. The reason for the differences in density values between the two types of DES is that the molecular weight of ChDHCit (295.29 g/mol) is greater than that of ChCl (139.62 g/mol).

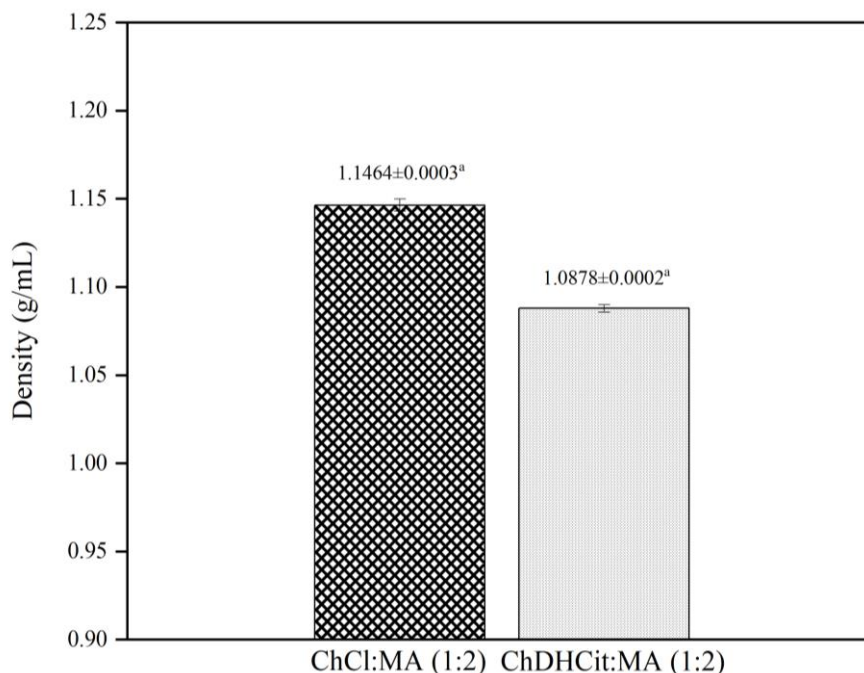


Figure 9. Densities of ChCl:MA and ChDHCit:MA at 25°C.

Higher-molecular-weight HBAs or HBDs tend to increase the overall mass of the DES, which could intuitively suggest an increase in density. However, the relationship between molecular weight and density in DES systems is not straightforward because of the complex interplay between molecular size, extent of hydrogen bonding, and resultant volume occupied by the DES. As mentioned by Sinclair et al. [80], the presence of bulky HBA molecules can disrupt the compactness of the molecular packing within the DES structure because of the increased volume occupied, formation of HBD-HBD aggregates, and the prevalence of HBD-anion hydrogen bonds. In this study, ChDHCit had a lower density which is probably due to the asymmetrical dihydrogen citrate ion, which restricts the closer packing of the molecules, as explained in a previous viscosity study, in which ChCl:MA is more flexible and packed more tightly than ChDHCit:MA. This study was compared with that of Ibrahim et al. [67], who studied the physicochemical properties of DES comprising ethylene-glycol-based HBAs. They observed that the densities decreased in the following order: methyl-triphenyl-ethanol-ammonium chloride > benzyl-triphenyl-phosphonium bromide > ChCl > N, N-diethyl-triphenyl-phosphonium bromide < tetra-n-butyl-ammonium bromide. According to Fuad et al. [57] and Sharma et al. [81], increasing the carbon chain length of HBA or HBD restricts closer packing within the DES systems. This leads to greater hindrance and fewer possible hydrogen-bonding interactions, thereby reducing the density of certain DES. The findings yield demonstrated that a smaller HBA size leads to a denser eutectic mixture.

The density of DES holds a vital part in determining their suitability for various applications, as it affects their solvation ability and interactions with different substances. High-density DESs are particularly advantageous in applications that require efficient phase separation and the ability to dissolve denser materials. For instance, in the oil and gas industry, high-density DES are preferred for separation processes, such as dearomatization, desulfurisation, and purification of biodiesel, as their density aids in the effective separation of components based on their densities [82]. Another example that necessitates a high density of DES is in the extraction of pectin. An increased density of DES can enhance the separation of pectin from the solid matrix, resulting in a higher yield of extracted pectin. This phenomenon can be attributed to the superior ability of denser solvents to dissolve and transport pectin away from the plant material, thereby underscoring the relationship between the density of DES and the extraction process [77]. On the other hand, low-density DES find applications in areas where lighter solvents are required for effective processing, or where the buoyancy of solutes is a factor. For example, in analytical chemistry, low-density DES are utilised as effective extractants for the isolation of both hydrophobic and hydrophilic analytes from various samples, where their lower density can be beneficial for liquid-liquid extraction processes [83]. Furthermore, in the electrochemistry field, DESs with lower densities are preferred for applications, for example, electrolytes in batteries and supercapacitors because they can lower the overall weight of the device and enhance its portability and efficiency [84, 85]. In summary, the suitability of

high- or low-density DESs for certain applications is determined by the specific requirements of the process, including the need for phase separation, density of materials to be dissolved, and desired physical properties of the end product.

Surface Tension

The idea of the surface tension in a liquid refers to the force per unit length acting on its surface. In the context of DES, the surface tension is influenced by the hydrogen bonding between HBA as well as HBD. As displayed in **Figure 10**, the surface tensions of both DES were comparable, but that of ChDHCit:MA (49.903 ± 0.376^a mN/m) was slightly greater compared to that of ChCl:MA (48.944 ± 0.140^a mN/m). These differences may be related to the size of the dihydrogen citrate anion which was larger than that of the chloride anion. The large anions increase the surface area by incorporating more hydroxyl groups, which forms stronger hydrogen bonds with MA, resulting in cohesive forces. This enhances the surface's ability to generate stronger mutual attractive forces that counteract external forces, making the surface molecules more resistant to breakage. This idea was corroborated by Guan et al. [86], who integrated the density gradient

with perturbed chain statistical associating fluid theory as a model to achieve a comprehensive understanding of the phenomenon. They mentioned that the large anion of HBA within the DES system led to enhanced interfacial interactions and the resultant increase in the energy needed to disrupt the DES liquid's surface layer.

In addition, the surface tension is closely associated to the viscosity of DES, where a more viscous fluid tends to have a higher surface tension owing to the increased intermolecular forces at the surface and vice versa [87]. Because the viscosity of ChDHCit:MA is greater than that of ChCl:MA, the resulting surface tension is also high. The high viscosity of ChDHCit:MA means the molecules exhibit lower mobility, leading to a non-uniform distribution at the liquid-air interface. Due to this reason, the cohesive forces were enhanced and contributed to its high surface tension. Nunes et al. [88] further supported this relationship. They reported that menthol-octanoic acid based DES exhibited high and low viscosities of 8.81 mPa.s (at 25°C) and 3.51 mPa.s (at 55°C), respectively, which correlated with their high surface tension of 23.32 mN/m and 20.44 mN/m. It can therefore be anticipated that the viscosity of DES affects its surface tension, as these two properties are interconnected.

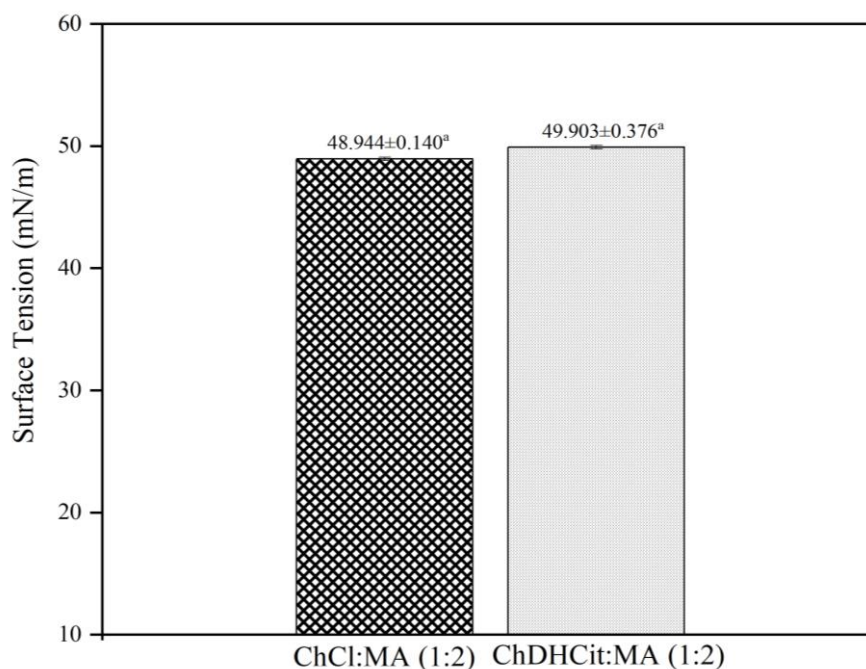


Figure 10. Surface tension of ChCl:MA and ChDHCit:MA at 25°C.

Compared to the study conducted by Omar and Sadeghi [89], the surface tension of pyrogallol-based HBAs, including ChCl, n-dodecyl-trimethylammonium bromide (n-DDTMAB), tetraethylammonium bromide (TEAB), tetrapropylammonium bromide (TPAB), and tetrabutylammonium bromide (TBAB), decreased in the following order: [ChCl:PY] > [TEAB:PY] > [TPAB:PY] > [TBAB:PY] > [n-DDTMAB:PY]. They noted that the length of the alkyl chain in HBA significantly influenced this trend of decreasing surface tension, indicating that longer alkyl chains resulted in higher surface tension. In comparison, Chen et al. [90] reported the surface tension of ethylene glycol (EG) based ChCl and ChBr to be 49.4 and 48.3 mN/m, respectively. They stressed that the higher surface tension of ChCl:EG than that of ChBr:EG could be attributed to the superior capacity of Cl⁻ anions to form stronger electrostatic interactions than Br⁻ anions, due to the smaller radius and greater electronegativity of Cl within the halogen group of the periodic table. Therefore, it may be concluded that the surface tension of the DES is affected by the alkyl chain length, electronegativity, and size of the HBA anions.

Ionic Conductivity

The ionic conductivity with respect to a DES is a measure of its ability to transmit electric current because of the presence of ions within its composition. The ionic conductivities of ChCl:MA and ChDHCit:MA were experimentally determined at 25°C. As depicted in **Figure 11**, the ionic conductivity of ChCl:MA (954 ± 5.292^a $\mu\text{S}/\text{cm}$) was greater than the ionic conductivity of ChDHCit:MA (41.67 ± 1.528^a $\mu\text{S}/\text{cm}$). This can be associated to the smaller size of the Cl⁻ anion in comparison to the C₆H₅O₇⁻ anion. Therefore, the smaller ionic radius of the Cl⁻ anion results in a shift of the eutectic point towards higher salt contents,

leading to increased ionic conductivity. Additionally, the hydrogen bonding strength and viscosity of ChCl:MA were lower than those of ChDHCit:MA, indicating that the ability of the Cl⁻ anions to move more freely was more pronounced than that of the C₆H₅O₇⁻ anion.

As compared with the study conducted by Sedghamiz and Raeissi [91], the values of ionic conductivities of ethylene glycol (EG) with different HBA based DESs was increased as the following order: NaCl-EG (4.73 mS/cm) < NaBr-EG (6.92 mS/cm) < NaI-EG (7.81 mS/cm). They attributed the increasing trend of ionic conductivity with respect to the prepared DES to the increased size of the halogen atoms, which means that the valence electrons are far from the nucleus, enabling them to move more freely. The size of the HBA used and the mobility of the ions within the system clearly influence the ionic conductivity of the DES. Undoubtedly, the preparation of a high-ionic-conductivity DES may be achieved by selecting smaller-sized HBA with a significantly simpler structure, which is advantageous for lowering its viscosity. The ionic conductivity of DES is pivotal in various industrial applications, including batteries and extraction processes. In the context of batteries and supercapacitors, high ionic conductivity is essential for efficient charge transport, as it enables ions to move more freely [92]. Furthermore, in pectin extraction, as noted by Alamineh [93], the elevated ionic conductivity of DES can enhance the extraction process by improving solvent penetration into plant tissues, thereby increasing extraction yields. Consequently, the implementation of a DES with high ionic conductivity presents an effective strategy for developing electrochemical devices and augmenting the pectin extraction process.

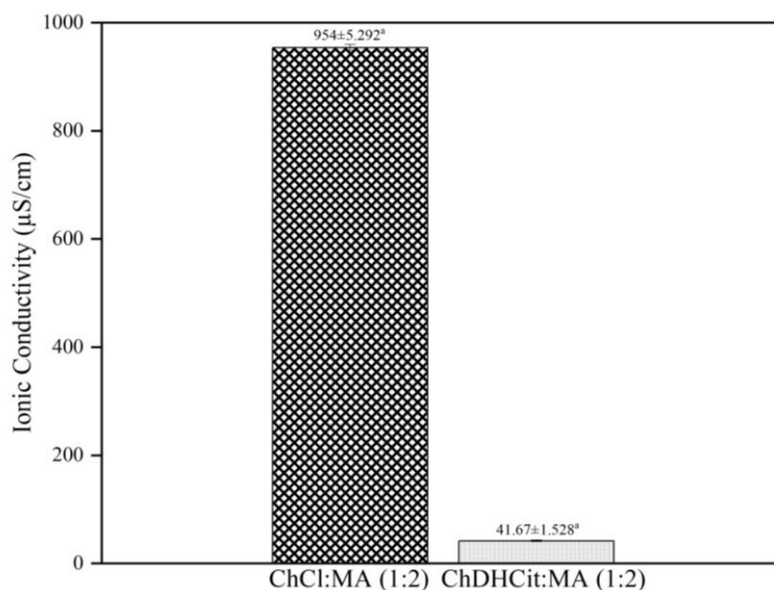


Figure 11. Ionic conductivities of ChCl:MA and ChDHCit:MA mixtures at 25°C.

Table 4. Solubilities of ChCl:MA and ChDHCit:MA at 25°C.

Solvent (Polarity Index)	ChCl:MA (1:2)	ChDHCit:MA (1:2)
Hexane (0.009)	non-miscible	non-miscible
Chloroform (0.259)	non-miscible	non-miscible
DMSO (0.444)	miscible	miscible
Acetic acid (0.648)	miscible	miscible
Ethanol (0.654)	miscible	miscible
Methanol (0.762)	miscible	miscible
Water (1.00)	miscible	miscible

Polarity

In chemical bonding, polarity is the unequal distribution of electrical charge over atoms, owing to the different electronegativities of the elements. Polarity is linked to solubility through the "like dissolve like" theory, which states that polar substances dissolve in polar solvents and vice versa. Hence, the polarities of ChCl:MA and ChDHCit:MA could be predicted by dissolving them in a wide range of solvents, as summarised in **Table 4**. The results showed that both the DES had a wide range of solubilities. DES are soluble in solvents with a polarity index above 0.444, such as dimethyl sulfoxide (DMSO), acetic acid, ethanol, methanol, and water. The DESs were not dissolved (non-miscible) in non-polar solvents such as hexane and chloroform, with polarity indices ranging from 0.009 to 0.2059. DMSO is a non-polar solvent, but the existence of a positive charge on sulphur and a negative charge on oxygen causes it to interact with the DES and dissolve them together. Therefore, ChCl:MA and ChDHCit:MA are hydrophilic DES that can be used as media for the extraction of polar compounds and biopolymers. The polarity of DES influences their efficacy in extracting both polar and non-polar compounds. For instance, Shafie et al. [17] synthesised a polar DES consisting of choline chloride and citric acid for the extraction of pectin from *Averrhoa bilimbi*, achieving a yield of 14.4%. This observation suggests that the presence of hydroxyl or carboxylic acid groups, acting as hydrogen bond donors (HBD), typically results in the formation of polar DES. Such polar DES exhibit the capacity to create strong interactions, including hydrogen bonds and dipole-dipole interactions, with polar solute molecules. Consequently, these interactions are believed to facilitate the effective solubilisation of polar molecules. In the context of non-polar DES, these solvents are specifically formulated to interact effectively with non-polar compounds. For instance, Srivastava et al. [94] employed a non-polar DES comprising acetic acid and n-decanoic acid in a molar ratio of 1:2. This particular composition imparts a polarity to the prepared DES that is akin to that of chloroform, a widely recognised non-polar solvent, thus rendering it proficient in the extraction of non-polar phytochemicals. The interactions between the non-polar DES and non-polar compounds occur via

van der Waals forces, which subsequently facilitate the solubilisation of these non-polar compounds. Through these interactions, the authors successfully extracted scopotelin, rutin and aegeline as non-polar phytochemicals. Therefore, to effectively target and extract polar compounds, a polar DES is necessary, whereas for the targeting and extraction of non-polar compounds, a non-polar DES is required.

CONCLUSION

ChCl:MA and ChDHCit:MA were successfully prepared at a mole ratio of 1:2, indicating that the HBA and HBD used were compatible. This was validated by FTIR-ATR analysis, which showed that hydrogen bonding existed between HBAs and HBD through O-H stretching. Various HBAs had a notable impact on the physicochemical properties of the DES. The outcomes demonstrated that ChDHCit:MA had a higher T_m and surface tension, whereas ChCl:MA had a higher T_d , acidity, density and ionic conductivity. A lower viscosity caused ChCl:MA facilitates mass transfer effectively during the extraction process. Even though ChDHCit:MA have higher viscosity, they are also potential to be used as solvent extractor since heating can reduce their viscosity, as it did not easily decompose. ChCl:MA is more thermally stable as its T_d is higher than ChDHCit:MA. Both DES are polar and soluble in water, as well as semi-polar and highly polar in organic solvents. Consequently, both DES can function as solvent extractors for the recovery of natural products like pectin and polysaccharides.

ACKNOWLEDGEMENT

The authors acknowledge facilities support from the Universiti Teknologi MARA and scholarship from MyBrainSc 2023 from the Ministry of High Education (MOHE) of Malaysia.

REFERENCES

1. Lei, Z., Chen, B., Koo, Y. M. and MacFarlane, D. R. (2017) Introduction: ionic liquids. *Chemical Reviews*, **117**(10), 6633–6635.
2. Shah, F. U., An, R. and Muhammad, N. (2020) Properties and applications of ionic liquids in

- energy and environmental science. *Frontiers in Chemistry*, **8**, 627213.
3. Fliieger, J. and Fliieger, M. (2020) Ionic liquids toxicity—benefits and threats. *International Journal of Molecular Sciences*, **21**(17), 6267.
 4. Ghandi, K. (2014) A review of ionic liquids, their limits, and applications. *Green and Sustainable Chemistry*, **4**(1), 43349.
 5. Shamsuri, A. A., and Abdullah, D. K. (2011) Ionic liquids: Preparations and limitations. *Makara Journal of Science*, **14**(2), 19.
 6. Smith, E. L., Abbott, A. P. and Ryder, K. S. (2014) Deep eutectic solvents (DESs) and their applications. *Chemical reviews*, **114**(21), 11060–11082.
 7. Płotka-Wasyłka, J., De la Guardia, M., Andruch, V. and Vilková, M. (2020) Deep eutectic solvents vs ionic liquids: Similarities and differences. *Microchemical Journal*, **159**, 105539.
 8. Bajpai, P. (2021) Deep eutectic solvents for pretreatment of lignocellulosic biomass. *Singapore: Springer*, 2191–5318.
 9. Ijardar, S. P., Singh, V. and Gardas, R. L. (2022) Revisiting the physicochemical properties and applications of deep eutectic solvents. *Molecules*, **27**(4), 1368.
 10. Makoś, P., Słupek, E. and Gębicki, J. (2020) Hydrophobic deep eutectic solvents in micro-extraction techniques—A review. *Microchemical Journal*, **152**, 104384.
 11. Cheng, H. and Qi, Z. (2021) Applications of deep eutectic solvents for hard-to-separate liquid systems. *Separation and Purification Technology*, **274**, 119027.
 12. Lane, T. R., Harris, J., Urbina, F. and Ekins, S. (2023) Comparing LD50/LC50 machine learning models for multiple species. *ACS Chemical Health & Safety*, **30**, 83–97.
 13. Marcus, Y. and Marcus, Y. (2019) Applications of deep eutectic solvents. *Springer International Publishing*, 111–151.
 14. Hansen, B. B., Spittle, S., Chen, B., Poe, D., Zhang, Y., Klein, J. M. and Sangoro, J. R. (2020) Deep eutectic solvents: A review of fundamentals and applications. *Chemical Reviews*, **121**(3), 1232–1285.
 15. Hayyan, M. (2023) Versatile applications of deep eutectic solvents in drug discovery and drug delivery systems: Perspectives and opportunities. *Asian Journal of Pharmaceutical Sciences*, **18**(2), 100780.
 16. Chabib, C. M., Ali, J. K., Abi Jaoude, M., Alhseinat, E., Adeyemi, I. A., and Al Nashef, I. M. (2022) Application of deep eutectic solvents in water treatment processes: A review. *Journal of Water Process Engineering*, **47**, 102663.
 17. Shafie, M. H., Yusof, R. and Gan, C. Y. (2019) Synthesis of citric acid monohydrate-choline chloride based deep eutectic solvents (DES) and characterization of their physicochemical properties. *Journal of Molecular Liquids*, **288**, 111081.
 18. Zhan, A., Niu, D., Li, K. and Li, J. (2023) Characterization of some sucrose-based deep eutectic solvents and their effect on the solubility of piroxicam. *Journal of Molecular Liquids*, **377**, 121556.
 19. Craveiro, R., Aroso, I., Flammia, V., Carvalho, T., Viciosa, M. T., Dionísio, M. and Paiva, A. (2016) Properties and thermal behavior of natural deep eutectic solvents. *Journal of Molecular Liquids*, **215**, 534–540.
 20. Sai, M. S. N., De, D., Gariya, D. and Satyavathi, B. (2022) Thermophysical characterization of terpenoid based hydrophobic deep eutectic solvent and its Vapour-Liquid equilibrium studies with furfural. *Journal of Molecular Liquids*, **364**, 120056.
 21. Shishov, A., Makoś-Chełstowska, P., Bulatov, A. and Andruch, V. (2022) Deep eutectic solvents or eutectic mixtures? Characterization of tetrabutylammonium bromide and nonanoic acid mixtures. *The Journal of Physical Chemistry B*, **126**(21), 3889–3896.
 22. Skulcova, A., Russ, A., Jablonsky, M. and Sima, J. (2018) The pH behavior of seventeen deep eutectic solvents. *BioResources*, **13**(3), 5042–5051.
 23. Aroso, I. M., Paiva, A., Reis, R. L., and Duarte, A. R. C. (2017) Natural deep eutectic solvents from choline chloride and betaine—Physicochemical properties. *Journal of Molecular Liquids*, **241**, 654–661.
 24. Yusof, R., Abdulmalek, E., Sirat, K. and Rahman, M. B. A. (2014) Tetrabutylammonium bromide (TBABr)-based deep eutectic solvents (DESs) and their physical properties. *Molecules*, **19**(6), 8011–8026.
 25. Silva, J. M., Silva, E., Reis, R. L. and Duarte, A. R. C. (2019) A closer look in the antimicrobial properties of deep eutectic solvents based on fatty acids. *Sustainable Chemistry and Pharmacy*, **14**, 100192.

- 169 Mohammad Amin Wan Chik, Muhammad Hakimin Shafie, Roziana Mohamed Hanaphi and Rizana Yusof
- Unlocking Choline Dihydrogen Citrate as a New Potential Hydrogen Bond Acceptor Replacing Choline Chloride in Malonic Acid-Based Deep Eutectic Solvent Formulation
26. Shumilin, I., Tanbuz, A. and Harries, D. (2023) Deep Eutectic Solvents for Efficient Drug Solvation: Optimizing Composition and Ratio for Solubility of β -Cyclodextrin. *Pharmaceutics*, **15**(5), 1462.
 27. Turiel, E., Díaz-Álvarez, M. and Martín-Esteban, A. (2024) Natural deep eutectic solvents as sustainable alternative for the Ultrasound-Assisted extraction of triazines from agricultural soils. *Microchemical Journal*, **196**, 109675.
 28. Inayat, S., Ahmad, S. R., Awan, S. J., Nawshad, M. and Ali, Q. (2023) In vivo and in vitro toxicity profile of tetrabutylammonium bromide and alcohol-based deep eutectic solvents. *Scientific Reports*, **13**(1), 1777.
 29. Mulia, K., Krisanti, E., Terahadi, F. and Putri, S. (2015) Selected natural deep eutectic solvents for the extraction of α -mangostin from mangosteen (*Garcinia mangostana* L.) pericarp. *International Journal of Technology*, **6**(7), 1211–1220.
 30. Thorat, G. M., Jadhav, H. S., Roy, A., Chung, W. J. and Seo, J. G. (2018) Dual role of deep eutectic solvent as a solvent and template for the synthesis of octahedral cobalt vanadate for an oxygen evolution reaction. *ACS Sustainable Chemistry & Engineering*, **6**(12), 16255–16266.
 31. Gautam, R., Kumar, N. and Lynam, J. G. (2020) Theoretical and experimental study of choline chloride-carboxylic acid deep eutectic solvents and their hydrogen bonds. *Journal of Molecular Structure*, **1222**, 128849.
 32. Busato, M., Mannucci, G., Di Lisio, V., Martinelli, A., Del Giudice, A., Tofoni, A. and D'Angelo, P. (2022) Structural Study of a Eutectic Solvent Reveals Hydrophobic Segregation and Lack of Hydrogen Bonding between the Components. *ACS Sustainable Chemistry & Engineering*, **10**(19), 6337–6345.
 33. González-Rivera, J., Pelosi, C., Pulidori, E., Duce, C., Tiné, M. R., Ciancaleoni, G. and Bernazzani, L. (2022) Guidelines for a correct evaluation of Deep Eutectic Solvents thermal stability. *Current Research in Green and Sustainable Chemistry*, **5**, 100333.
 34. Zhang, Y. and Rempel, C. (2012) Retrogradation and antiplasticization of thermoplastic starch. *Thermoplastic Elastomers*, **118119**, 117–134.
 35. Gajardo-Parra, N. F., Lubben, M. J., Winnert, J. M., Leiva, Á., Brennecke, J. F. and Canales, R. I. (2019) Physicochemical properties of choline chloride-based deep eutectic solvents and excess properties of their pseudo-binary mixtures with 1-butanol. *The Journal of Chemical Thermodynamics*, **133**, 272–284.
 36. Delgado-Mellado, N., Larriba, M., Navarro, P., Rigual, V., Ayuso, M., García, J. and Rodríguez, F. (2018) Thermal stability of choline chloride deep eutectic solvents by TGA/FTIR-ATR analysis. *Journal of Molecular Liquids*, **260**, 37–43.
 37. Florindo, C., Oliveira, F. S., Rebelo, L. P. N., Fernandes, A. M. and Marrucho, I. M. (2014) Insights into the synthesis and properties of deep eutectic solvents based on cholinium chloride and carboxylic acids. *ACS Sustainable Chemistry & Engineering*, **2**(10), 2416–2425.
 38. Marchel, M., Cieśliński, H. and Boczkaj, G. (2022) Thermal instability of choline chloride-based deep eutectic solvents and its influence on their toxicity— important limitations of DESs as sustainable materials. *Industrial & Engineering Chemistry Research*, **61**(30), 11288–11300.
 39. Rodriguez Rodriguez, N., van den Bruinhorst, A., Kollau, L. J., Kroon, M. C. and Binnemans, K. (2019) Degradation of deep-eutectic solvents based on choline chloride and carboxylic acids. *ACS Sustainable Chemistry & Engineering*, **7**(13), 11521–11528.
 40. Al-Dawsari, J. N., Bessadok-Jemai, A., Wazeer, I., Mokraoui, S., AlMansour, M. A. and Hadj-Kali, M. K. (2020) Fitting of experimental viscosity to temperature data for deep eutectic solvents. *Journal of Molecular Liquids*, **310**, 113127.
 41. Shishov, A., Pochivalov, A., Nugbienyo, L., Andruch, V. and Bulatov, A. (2020) Deep eutectic solvents are not only effective extractants. *TrAC Trends in Analytical Chemistry*, **129**, 115956.
 42. Antariksa, N. F., Yamada, T. and Kimizuka, N. (2021) High seebeck coefficient in middle-temperature thermocell with deep eutectic solvent. *Scientific Reports*, **11**(1), 11929.
 43. Zec, N., Mangiapia, G., Zheludkevich, M. L., Busch, S. and Moulin, J. F. (2020) Revealing the interfacial nanostructure of a deep eutectic solvent at a solid electrode. *Physical Chemistry Chemical Physics*, **22**(21), 12104–12112.
 44. Pal, S., Roy, R. and Paul, S. (2020) Potential of a natural deep eutectic solvent, glyceline, in the thermal stability of the Trp-Cage mini-protein. *The Journal of Physical Chemistry B*, **124**(35), 7598–7610.
 45. Majid, M. F., Zaid, H. F. M., Kait, C. F., Abd Ghani, N. and Jumbri, K. (2019) Mixtures of tetrabutylammonium chloride salt with different glycol structures: Thermal stability and functional groups characterizations. *Journal of Molecular Liquids*, **294**, 111588.

46. Mero, A., Koutsoumpos, S., Giannios, P., Stavrakas, I., Moutzouris, K., Mezzetta, A. and Guazzelli, L. (2023) Comparison of physicochemical and thermal properties of choline chloride and betaine-based deep eutectic solvents: The influence of hydrogen bond acceptor and hydrogen bond donor nature and their molar ratios. *Journal of Molecular Liquids*, **377**, 121563.
47. Alvarez, M. S., Longo, M. A., Deive, F. J. and Rodriguez, A. (2021) Synthesis and characterization of a lipase-friendly DES based on cholinium dihydrogen phosphate. *Journal of Molecular Liquids*, **340**, 117230.
48. Jablonsky, M., Skulcova, A., Haz, A., Sima, J. and Majová, V. (2018) Long-term isothermal stability of deep eutectic solvents. *BioResources*, **13(4)**, 7545–7559.
49. Pal, S., Roy, R., Paul, S. (2020) Potential of a natural deep eutectic solvent, glyceline, in the thermal stability of the trp-cage mini-protein. *Journal of Physical Chemistry B*, **124**, 7598–7610.
50. Lin, X., Liu, Y., Wang, R., Dai, J. and Zhang, J. (2024) Extraction of pectins from renewable grapefruit (*Citrus paradisi*) peels using deep eutectic solvents and analysis of their structural and physicochemical properties. *International Journal of Biological Macromolecules*, **254**, 127785.
51. Hammond, O. S., Edler, K. J., Bowron, D. T. and Torrente-Murciano, L. (2017) Deep eutectic-solvothermal synthesis of nanostructured ceria. *Nature Communications*, **8(1)**, 14150.
52. Sazali, A. L., AlMasoud, N., Amran, S. K., Alomar, T. S., Pa'ee, K. F., El-Bahy, Z. M. and Chuah, L. F. (2023) Physicochemical and thermal characteristics of choline chloride-based deep eutectic solvents. *Chemosphere*, **338**, 139485.
53. Zhang, Y., Cao, Y. and Wang, H. (2020) Multi-interactions in ionic liquids for natural product extraction. *Molecules*, **26(1)**, 98.
54. AlOmar, M. K., Hayyan, M., Alsaadi, M. A., Akib, S., Hayyan, A. and Hashim, M. A. (2016) Glycerol-based deep eutectic solvents: Physical properties. *Journal of Molecular Liquids*, **215**, 98–103.
55. Du, C. Y., Wang, W., Wang, N., Pang, S. F. and Zhang, Y. H. (2021) Impact of ambient relative humidity and acidity on chemical composition evolution for malonic acid/calcium nitrate mixed particles. *Chemosphere*, **276**, 130140.
56. Nia, N. N. and Hadjmohammadi, M. R. (2021) Amino acids-based hydrophobic natural deep eutectic solvents as a green acceptor phase in two-phase hollow fiber-liquid microextraction for the determination of caffeic acid in coffee, green tea, and tomato samples. *Microchemical Journal*, **164**, 106021.
57. Fuad, F. M. and Nadzir, M. M. (2022) The formulation and physicochemical properties of betaine-based natural deep eutectic solvent. *Journal of Molecular Liquids*, **360**, 119392.
58. Teles, A. R. R., Capela, E. V., Carmo, R. S., Coutinho, J. A., Silvestre, A. J. and Freire, M. G. (2017) Solvatochromic parameters of deep eutectic solvents formed by ammonium-based salts and carboxylic acids. *Fluid Phase Equilibria*, **448**, 15–21.
59. Zhang, W., Cheng, S., Zhai, X., Sun, J., Hu, X., Pei, H. and Chen, G. (2020) Green and efficient extraction of polysaccharides from *Poria cocos* FA Wolf by deep eutectic solvent. *Natural Product Communications*, **15(2)**, 1934578X19900708.
60. Liew, S. Q., Ngoh, G. C., Yusoff, R. and Teoh, W. H. (2018) Acid and Deep Eutectic Solvent (DES) extraction of pectin from pomelo (*Citrus grandis* (L.) Osbeck) peels. *Biocatalysis and Agricultural Biotechnology*, **13**, 1–11.
61. Neckebroeck, B., Verkempinck, S. H. E., Van Audenhove, J., Bernaerts, T., de Wilde d'Estmael, H., Hendrickx, M. E. and Van Loey, A. M. (2021) Structural and emulsion stabilizing properties of pectin rich extracts obtained from different botanical sources. *Food Research International*, **141**, 110087.
62. White, P. B., Wang, T., Park, Y. B., Cosgrove, D. J. and Hong, M. (2014) Water–polysaccharide interactions in the primary cell wall of *Arabidopsis thaliana* from polarization transfer solid-state NMR. *Journal of the American Chemical Society*, **136(29)**, 10399–10409.
63. Lin, J., Xiang, H., Sun-Waterhouse, D., Cui, C. and Wang, W. (2022) Deep eutectic solvents and alkaline extraction of protein from seabuckthorn seed meal: a comparison study. *Food Science and Human Wellness*, **11(4)**, 1028–1035.
64. Lapeña, D., Lomba, L., Artal, M., Lafuente, C. and Giner, B. (2019) Thermophysical characterization of the deep eutectic solvent choline chloride: ethylene glycol and one of its mixtures with water. *Fluid Phase Equilibria*, **492**, 1–9.
65. Pan, Z., Bo, Y., Liang, Y., Lu, B., Zhan, J., Zhang, J. and Zhang, J. (2021) Intermolecular interactions in natural deep eutectic solvents and their effects on the ultrasound-assisted extraction of artemisinin from *Artemisia annua*. *Journal of Molecular Liquids*, **326**, 115283.

- 171 Mohammad Amin Wan Chik, Muhammad Hakimin Shafie, Roziana Mohamed Hanaphi and Rizana Yusof
66. Dias, M. C. G. C., Farias, F. O., Gaioto, R. C., Kaspchak, E., da Costa, M. C., Igarashi-Mafra, L. and Mafra, M. R. (2022) Thermophysical characterization of deep eutectic solvents composed by D-sorbitol, xylitol or D (+) xylose as hydrogen bond donors. *Journal of Molecular Liquids*, **354**, 118801.
67. Ibrahim, R. K., Hayyan, M., AlSaadi, M. A., Ibrahim, S., Hayyan, A. and Hashim, M. A. (2019) Physical properties of ethylene glycol-based deep eutectic solvents. *Journal of Molecular Liquids*, **276**, 794–800.
68. Fan, S., Fang, F., Lei, A., Zheng, J. and Zhang, F. (2021) Effects of salts on structural, physicochemical and rheological properties of low-methoxyl pectin/sodium caseinate complex. *Foods*, **10**(9), 2009.
69. Savi, L. K., Carpiné, D., Waszczynskyj, N., Ribani, R. H. and Haminiuk, C. W. I. (2019) Influence of temperature, water content and type of organic acid on the formation, stability and properties of functional natural deep eutectic solvents. *Fluid Phase Equilibria*, **488**, 40–47.
70. Mannu, A., Blangetti, M., Baldino, S. and Prandi, C. (2021) Promising technological and industrial applications of deep eutectic systems. *Materials*, **14**(10), 2494.
71. García, G., Aparicio, S., Ullah, R. and Atilhan, M. (2015) Deep eutectic solvents: physicochemical properties and gas separation applications. *Energy & Fuels*, **29**(4), 2616–2644.
72. Shishov, A., Pochivalov, A., Dubrovsky, I. and Bulatov, A. (2023) Deep eutectic solvents with low viscosity for automation of liquid-phase microextraction based on lab-in-syringe system: separation of Sudan dyes. *Talanta*, **255**, 124243.
73. Picchio, M. L., Minudri, D., Mantione, D., Criado-Gonzalez, M., Guzmán-González, G., Schmarsow, R. and Mecerreyes, D. (2022) Natural deep eutectic solvents based on choline chloride and phenolic compounds as efficient bioadhesives and corrosion protectors. *ACS Sustainable Chemistry & Engineering*, **10**(25), 8135–8142.
74. Devi, M., Moral, R., Thakuria, S., Mitra, A. and Paul, S. (2023) Hydrophobic deep eutectic solvents as greener substitutes for conventional extraction media: Examples and techniques. *ACS omega*, **8**(11), 9702–9728.
75. Ijardar, S. P. (2020) Deep eutectic solvents composed of tetrabutylammonium bromide and PEG: Density, speed of sound and viscosity as a function of temperature. *The Journal of Chemical Thermodynamics*, **140**, 105897.
- Unlocking Choline Dihydrogen Citrate as a New Potential Hydrogen Bond Acceptor Replacing Choline Chloride in Malonic Acid-Based Deep Eutectic Solvent Formulation
76. Lin, H., Gong, K., Ying, W., Chen, D., Zhang, J., Yan, Y. and Peng, X. (2019) CO₂-philic separation membrane: deep eutectic solvent filled graphene oxide nanoslits. *Small*, **15**(49), 1904145.
77. Wan Chik, M. A., Yusof, R., Shafie, M. H. and Mohamed Hanaphi, R. (2024) Extraction optimisation and characterisation of Artocarpus integer peel pectin by malonic acid-based deep eutectic solvents using response surface methodology. *International Journal of Biological Macromolecules*, **280**, 135737.
78. Bušić, V., Molnar, M., Tomičić, V., Božanović, D., Jerković, I. and Gašo-Sokač, D. (2022) Choline chloride-based deep eutectic solvents as green effective medium for quaternization reactions. *Molecules*, **27**(21), 7429.
79. Gontrani, L., Plechkova, N. V. and Bonomo, M. (2019) In-depth physico-chemical and structural investigation of a dicarboxylic acid/choline chloride natural deep eutectic solvent (NADES): a spotlight on the importance of a rigorous preparation procedure. *ACS Sustainable Chemistry & Engineering*, **7**(14), 12536–12543.
80. Sinclair, N., Savinell, R. F. and Wainright, J. S. (2022) Understanding Hydrogen Bonding Effects on the Reversibility and Redox Potential of Redox Organic Molecules in Deep Eutectic Solvents. In *Electrochemical Society Meeting Abstracts 241*, *The Electrochemical Society, Inc.*, **1**, 139-139, July, 2022).
81. Sharma, R., Athira, K. K., Gardas, R. L., Malek, N. and Ijardar, S. P. (2022) Physicochemical and acoustic characterization of binary mixtures of tetraalkylammonium bromide: PEG based DES and water. *Journal of Molecular Liquids*, **367**, 120386.
82. De Oliveira Vigier, K. and Jérôme, F. (2023) Editorial deep eutectic solvents. *Current Opinion in Green and Sustainable Chemistry*, **41**, 100805.
83. Figueroa, V. P. C. (2020) Physicochemical Study of Deep Eutectic Solvents Mixed with Alcohols: Effect of Temperature, Hydrogen Bond Donor and Alcohol Chain Length (Master's thesis, Pontificia Universidad Católica de Chile (Chile)).
84. Dangre, P. V., Borase, H. P., Gunde, M. C., Pethe, A. M. and Borkar, M. R. (2023) Deep eutectic solvents: Fundamental aspect, characterizations and applications. *Recent Advances in Drug Delivery and Formulation: Formerly Recent Patents on Drug Delivery & Formulation*, **17**(1), 3–12.
85. Abdollahzadeh, M., Khosravi, M., Hajipour Khire Masjidi, B., Samimi Behbahan, A., Bagherzadeh,

- A., Shahkar, A. and Tat Shahdost, F. (2022) Estimating the density of deep eutectic solvents applying supervised machine learning techniques. *Scientific Reports*, **12(1)**, 4954.
86. Guan, S., Li, Z., Xu, B., Wu, J., Han, J., Guan, T. and Li, K. (2023) Deep Eutectic Solvents with Excellent Catalytic Ability for Extractive and Oxidative Desulfurization under Room Temperature. *ACS Sustainable Chemistry & Engineering*, **11(16)**, 6292–6301.
87. Chen, H., Wang, A., Yan, C., Liu, S., Li, L., Wu, Q. and Yu, H. (2023) Study on the solubility of industrial lignin in choline chloride-based deep eutectic solvents. *Sustainability*, **15(9)**, 7118.
88. Nunes, R. J., Saramago, B. and Marrucho, I. M. (2019) Surface tension of dl-menthol: octanoic acid eutectic mixtures. *Journal of Chemical & Engineering Data*, **64(11)**, 4915–4923.
89. Omar, K. A. and Sadeghi, R. (2021) Novel deep eutectic solvents based on pyrogallol: synthesis and characterizations. *Journal of Chemical & Engineering Data*, **66(5)**, 2088-2095.
90. Chen, Y., Chen, W., Fu, L., Yang, Y., Wang, Y., Hu, X. and Mu, T. (2019) Surface tension of
- 50 deep eutectic solvents: effect of hydrogen-bonding donors, hydrogen-bonding acceptors, other solvents, and temperature. *Industrial & Engineering Chemistry Research*, **58(28)**, 12741–12750.
91. Sedghamiz, M. A. and Raeissi, S. (2018) Physical properties of deep eutectic solvents formed by the sodium halide salts and ethylene glycol, and their mixtures with water. *Journal of Molecular Liquids*, **269**, 694–702.
92. Schulz, A., Lunkenheimer, P., Loidl, A. (2024) Ionic conductivity of a lithium-doped deep eutectic solvent: glass formation and rotation-translation coupling. *Journal of Physical Chemistry B*, **128**, 3454–3462.
93. Alamineh, E. A. (2018) Extraction of pectin from orange peels and characterizing its physical and chemical properties. *American Journal of Applied Chemistry*, **6(2)**, 51–56.
94. Srivastava, R., Bhardwaj, N., Jain, S. K., Metya, A. K., Parambil, J. V. (2024) Unveiling the potential of acetic acid-based hydrophobic natural deep eutectic solvents for phytochemical extraction. *Journal of Molecular Liquids*, **408**, 125314.